AN INVESTIGATION OF DETACHED SHOCK WAVES

Thesis by

Bernard Walter Marschner

In Partial Fulfillment of the Requirements

for the Degree of Aeronautical Engineer

California Institute of Technology

Pasadena, California

1948

ABSTRACT

This investigation demonstrates an application of a flexible wall nozzle for testing in a supersonic wind tunnel. It is conservative to say that the versatility of this nozzle is such that it warrants the expenditure of time to carefully engineer a nozzle and incorporate it in the wind tunnel as a permanent part of the system. The gradients in the test section were kept within one percent of the calibrated Mach number, however, the gradients occurring over the bodies tested were only $\pm$ 0.2 percent in Mach number.

The conditions existing on a finite cone with a vertex angle of 75° were investigated by considering the pressure distribution on the cone and the shape of the shock wave. The pressure distribution on the surface of the 75° cone when based on upstream conditions does not show any discontinuities at the theoretical attachment Mach number.

Both the angle of the shock wave and the pressure distribution of the 75° cone are in very close agreement with the theoretical values given in the Kopal report, (Ref. 3).

The location of the intersection of the sonic line with the surface of the cone and with the shock wave are given for the 75° cone. The blocking characteristics of the GALCIT supersonic wind tunnel were investigated with a series of 60° cones.

ACKNOWLEDGMENTS

This investigation was conducted jointly with Mr. John Altseimer. Considerable advice and assistance were obtained from Mr. Henry T. Nagamatsu and Mr. Allen E. Puckett, for which the author wishes to express his appreciation.

LIST OF FIGURES

I. Introduction

The general objectives in this investigation were to demonstrate an application of a flexible wall supersonic nozzle, and to investigate the nature of the conditions occuring in the immediate vicinity of a cone shaped body with a detached shock wave.

The second objective provided a problem which would be a ready application of the flexible wall nozzle. It was desirable to cover a small Mach number range rather thoroughly which would have required a number of fixed nozzle blocks, and these various Mach number settings would be required to be essentially gradient free. The conditions on a rather steep cone with 75° total vertex angle are to be investigated both from the aspect of the pressure distribution of the face of the cone, as well as, the behaviour of the shock wave with regard to shape and location.

II. Equipment

The wind tunnel which was used for this investigation was the GALCIT 2.5" Supersonic Wind Tunnel, the details of which are completely described in a GALCIT publication, (Ref. 1).

In the place of the fixed nozzle blocks normally used, a flexible wall nozzle was used in this testing program. It was felt that by the use of such a nozzle, the desired Mach numbers could be obtained with good flow readily and easily. The nozzle was a two-dimensional type with both the upper and lower surfaces flexible. The flexible plates were made out of copper sheeting of .031 inch thickness. Each plate was supported by twenty-three jacks which were soldered to the plates through a pivioting connecting system. It would have been better if a stronger method of attaching the jacks to the plates other than soldering could been used, as this type of joint was quite weak and several jacks had to be resoldered during the testing program. However, the plate was too thin to use bolts as they would have disturbed the smooth surface of the test section. In the downstream portion of the nozzle the jack spacing was three-quarters of an inch, while in the upstream portion the spacing was one inch. The jacks were manually adjusted by means of thumb screws. The sealing of the flexible wall presented a rather difficult problem, as the thin plate prevented using the usual type of inflated seals. Instead a compromise type of seal consisting of a non-inflated rubber tube cemented to the flexible plate was used. The sealing action was accomplished by the pressing of the rubber tube under pressure from the glass side plates.

The nozzle contours were calculated by the method of characteristics following the procedure outlined by A. E. Puckett, (Ref. 2). No attempt was made to calculate the boundary layer corrections; however, based on previous experience with the wind tunnel a divergence of .0033 inches per inch was incorporated in the nozzle setting. The nozzle contour was set by the use of a calibration device which consisted of a leveling bar which served as a track for an Ames dial gauge arrangement that measured the nozzle contour above the track reference line. The nozzle was set to the calculated corrected nozzle shapes at each jack support point to $\pm$ .001 inch. The nozzle and the calibration setup are shown in Figs. 1 - 3.

For each nozzle setting a complete axial and wall pressure survey was made. A shock wave picture for a 20° cone was taken by the use of the schlieren apparatus and the wave angle was measured to obtain an initial estimate of the Mach number of the nozzle. This determination was only for preliminary use as the pressure calibration of the nozzle was closely examined and the Mach number determination made on the basis of this examination. A representative calibration of one of the nozzle settings is presented in Fig. 4, which illustrates the Mach number variations along the centerline of the nozzle. A serious effort was made to keep the Mach number variations in the test section to less than one percent. The schlieren surveys did not indicate the presence of any wavelets, but at several of the nozzle settings considerable difficulty was encountered with excessive Mach number gradients. These gradients were corrected by the use of very gradual nozzle shapes. The limitations in jack travel restricted the maximum Mach number that could be obtained with the flexible nozzle to about

1.9, so for the highest Mach number utilized in this program an existing solid nozzle block was used.

For the pressure models used in this program, it was necessary to resort to extremely small diameter cones, as it was desired to test at as low a supersonic Mach number as possible without encountering blocking troubles. Hence, on this basis a cone of 1/4 inch diameter was selected. Since a number of pressure measurements along the face of the cone were desired, it appeared that to make a model of such a small diameter with about seven pressure orifices would be a very difficult task. So an alternative approach was used in that for each pressure orifice a separate cone with only one orifice was used, so a total of seven cones were needed. In this way the models could be made easily. The locations of the pressure orifices are illustrated on one cone in Fig. 5, which in reality represents the location of the individual orifices on the seven cones. The pressure cones had a total vertex angle of 75°, this angle being chosen in order that several Mach numbers below the detachment Mach number could be investigated. The theoretical Mach number for the detachment of the shock wave on the 75° cone is 1.80, (Ref. 3). The limitations on the capacity of the compressor system limited the lowest Mach number that flow could be established to about 1.4.

A set of 60° cones from 1/4 inch to 1 inch diameter in 1/16 inch steps was utilized in the investigation of the size of cone required to block the test section. In addition a 45°, 90° cone and a blunt cylinder were used during the investigation. The blunt cylinder had a pressure orifice located in the center of the flat face. Schlieren pictures were taken of the cones by the spark

system with an exposure time of 1/500,000 second. The schlieren apparatus used in this investigation is described in the previously mentioned GALCIT publication, (Ref. 1).

III. Testing Procedure

a. Pressure measurements.

After the nozzle had been calibrated with the axial static pressure tube, the series of seven 75° cones were tested in the tunnel. Because of trouble with the drying agent in the dryers, very poor control of the relative humidity was available. The relative humidity in the tunnel system was quite high during this investigation running about twenty-five percent. Since the humidity was not constant, it was necessary to make the tunnel calibration, test the pressure models, and take the schlieren photographs in as short a time interval as possible, as changes in the humidity of the tunnel could cause shifts in the test section Mach number calibration.

In this supersonic wind tunnel the absolute setting of the angle of attack of the model is not easily determined, and since separate models were used for each pressure orifice location, particular care was necessary in setting each of the models at zero degrees of incidence to the flow direction. As the relative inclination of the model from an arbitrary setting could be measured easily and with a good degree of accuracy, each model was tested first with the orifice at the top for four positions of angle of attack and pressures recorded. Then the model was rotated until the orifice was at the bottom and the same angles being repeated with pressure readings being made at the four settings. An auxiliary plot was then made and examined for the angle setting

for which the bottom and top pressures were equal, this setting being used as the zero angle of attack position. This procedure was followed on each of the seven pressure cones for each Mach number run. The blunt cone was set at zero angle of attack and the stagnation pressure behind the detached shock wave recorded.

b. Shock wave study.

After setting the cone to be examined at zero degrees of incidence, a schlieren picture was taken. Photographs were taken for each cone at each Mach number. Other than the care exercised in setting the angle of attack of the models no special procedures were followed in this part of the investigation.

c. Blocking tests

At each Mach number the series of increasing diameter 60° cones were tested in the tunnel and observed by means of the schlieren apparatus. When a particular size of cone produced blocking a slightly different tunnel operating procedure was used. The tunnel upstream pressure was built up while downstream portion of the system was evacuated until a large excess of pressure difference was obtained. With this excess the tunnel was started to see if the blocking occured from excessive losses by trying to force the normal shock down into the diffuser. If it was not possible to maintain supersonic flow past this cone, it was considered to be the size of cone which produced blocking of the test section. At each Mach number setting the size of the actual test section was measured by means of an inside micrometer. At the onset of the program it was thought that the 1/16 inch step in the diameter of the 60° cones were small enough; however, it

might have been better to have had cones of 1/32 inch variation in the diameter.

IV. Reduction and Presentation of Data

a. Pressure measurements.

The pressure data obtained from the set of 75° cones are presented in reduced form in several different ways. The location of the pressure orifices was reduced to a non-dimensional form of $\frac{x'}{S}$, where x' is the distance along the face of the cone measured from the nose of the cone and S is the slant length of the cone measured from the nose of the cone to the corner junction with the cylindrical portion of the model. These dimensions are given in Fig. 5. The pressure data was reduced in two ways, the first was in terms of $\frac{P_x}{P_o}$ where P_x is the static pressure measured at a particular orifice location and P_o is the stagnation pressure in the settling chamber of the wind tunnel. The variation of $\frac{P_x}{P_o}$ with orifice location $\frac{x'}{S}$ for the Mach numbers investigated are presented in Figs. 6 - 12. The variation of $\frac{P_x}{P_o}$ at a given orifice location with Mach number is presented in Fig. 13. The orifice designated as number 8 is the orifice located on the face of the blunt cylinder.

The pressure data was also reduced in terms of $\frac{P_x}{P_o'}$, where for the Mach numbers at which the shock wave was detached P_o' was taken as the stagnation pressure measured behind the detached shock wave occurring on the blunt cylinder. For Mach numbers greater than 1.80, P_o' was computed from oblique shock wave relations using the wave angle that occurred on the cone as observed by the schlieren photographs. The variation of $\frac{P_x}{P_o'}$ with orifice location $\frac{x'}{S}$ for the different Mach numbers investigated are presented in Fig. 14 - 20.

The variation of $\frac{P_x}{P_o}$, at a given orifice location $\frac{x'}{S}$ with Mach number is presented in Fig. 21. The ratio of the stagnation pressure before and after passing through the detached shock wave on the blunt cylinder is compared with the ratio calculated by using the normal shock wave relations in Fig. 22.

b. Shock wave study.

A series of schlieren pictures of the 75° cone for the Mach number range investigated are presented in Figs. 23 - 28. The series of schlieren pictures for the blunt cylinder are presented in Figs. 29 - 34, for the Mach numbers investigated. A series of photographs of the 45°, 60°, 75°, 90°, and 180° cones at the representative Mach number of 1.71 are presented in Figs. 35 - 39.

Enlargements of the cone pictures were made and the wave angle variation along the waves were measured by means of a prism and a drafting machine. The variation of the wave angle with y/D, where y is the vertical distance measured from the axis of the cone and D is the diameter of the cone, is presented for the 75° cone in Figs. 40 - 46 and for the blunt cylinder in Figs. 47 - 53. On these same figures the variation of Mach number behind the shock wave as determined from oblique shock wave relations with y/D, are presented. For the 75° cone the trace of the shock wave is presented for the six Mach numbers investigated on Fig. 54. Similarily the shock wave trace is presented in Fig. 55 for the blunt cylinder. For each of the three highest Mach numbers Mach numbers investigated the shock wave patterns of the five cones tested are shown in comparison in Figs. 56 - 58. The amount of detachment of the shock wave from the 75° cone and the blunt cylinder was measured. The variation of this distance in terms of s'/D, where s' is the distance from the

vertex of the cone to the outer face of the shock wave, with Mach number is presented for the two above mentioned cones in Figs. 59 and 60. The vertical location of the position for which Mach number 1 occurs behind the shock wave was obtained from the wave angle plots, and the variation of this distance with Mach number is presented for the 75° cone and the blunt cylinder in Fig. 61.

c. Blocking tests.

The cone size which produced blocking was determined by inspection of the schlieren pictures. A pair of representative schlieren photographs of the flow prior and after the blocking condition has occurred, are presented in Figs. 62 and 63. The physical dimension of the test section was measured, and the ratio of the cone area, which produced blocking, to the test section area for the range of Mach numbers investigated is presented in Fig. 64. For comparison the value of $\Delta A/A$ calculated from one dimensional theory is presented on the same figure.

V. Discussion of Results

Before discussing the data it is of interest to examine the analytical calculations to see what conditions exist on the cone. The calculated results were taken from the M.I.T. report, (Ref. 3). Unfortunately the cone chosen for this investigation was a poor choice as no data was given for this total vertex angle; however, cross plots were made and used in the comparison. The conditions existing on the face of the cone are illustrated clearly in Fig. 65. For the 75° cone the Mach number at which the shock wave attaches to the cone is seen to be 1.80. The free stream Mach number at which the Mach number behind the

oblique shock is unity is 1.93. The free stream Mach number at which the surface of the cone is first supersonic is M = 2.07. So for all of the Mach numbers utilized in this investigation the flow over the surface of the cone was subsonic. It is unfortunate that a nozzle with a Mach number of greater than 2.07 was not available in order that a test run could have been made in all of the three regions. With this as a background the other observed data will be discussed.

a. Pressure distribution.

With reference to Figs. 12 and 20, the fairing of the nose portion of the pressure distributions are open to some discussion and criticism. For the two lowest Mach numbers investigated, M = 1.41 and M = 1.49, the angle of the shock wave appears definitely to approach 90° at the axis of the cone. For this reason it was believed that the pressure existing at the nose of the cones for these two Mach numbers is the stagnation P_o' as obtained from the normal shock relations. An inspection of Figs. 23 and 24 illustrate the shock wave occurring for these two Mach numbers. The nose pressures were dashed faired from the last experimental point to the stagnation pressure existing behind a normal shock wave.

For the two highest Mach numbers investigated, M = 1.83 and M = 1.99, at which the shock wave was attached to the cone, the nose pressures were faired in as if conical conditions existed at the nose of the cone. The surface pressures calculated in the Kopal report (Ref. 3) are in very close agreement with the observed values and it was felt that this could be used as a justification for the fairing of the nose pressure for these two Mach numbers.

The nose pressures were not faired for either the M = 1.58

or M = 1.71 pressure distributions as it was felt that neither of the above mentioned procedures could be justified with the data available.

As the shock wave becomes attached at M = 1.80, the P_o' that was used in the reduction of the data for the P_x/P_o' plots for the M = 1.83 and M = 1.99 runs was calculated on the basis of P_o/P_o' obtained from oblique shock wave relations with an inclination of the shock wave obtained either from the calculated results on Fig. 65, or from the observed values presented in the wave angle plots as the agreement was almost exact. This change in P_o' is very pronounced in the P_x/P_o' data in Fig. 21. With the above discussed change in P_o', the variation of P_x/P_o' with Mach number would have a sharp discontinuity at the attachment Mach number, however, since there is considerable uncertainty on this method of calculating P_o' this region was faired in by a dashed curve in Fig. 21.

If we consider that our basis for computing P_o' is reasonably correct aside from this uncertain region, an inspection of the P_x/P_o' data should give an indication of the location of the sonic line on the surface of the cone. From Fig. 20, it can be seen that for the detached cases, i.e., M < 1.80, that P_x/P_o' critical occurs in the immediate vicinity of the corner junction. At the higher Mach numbers sonic velocity is reached before the corner junction. This intersection of the sonic line for the detached shock wave cases at the corner junction is in agreement with previously reported results, (Ref. 4).

Fig. 22 shows that the values of P_o' obtained from measurements on the blunt cylinder are in good agreement with the values

calculated from the normal shock wave relations.

b. Shock wave study.

The traces of the shock wave also indicate a gradual and smooth transition from the attached to the detached condition, as shown in Fig. 54, for the 75° cone. Of interest, is the location of the Mach number of one behind the shock wave for the 75° cone as this in conjunction with the result that the sonic line meets the cone at the corner gives a portion of the boundary of the subsonic region.

Inspection of the Fig. 59 illustrates the variation of the separation distance of the shock wave with Mach number for the 75° cone, while Fig. 60 illustrates the same thing for the blunt cylinder. This data is not to be considered accurate as it was measured from photographs and in this type of measuring it is difficult to obtain a high degree of accuracy.

Although the subsonic region, in general, can be determined for the 75° cone from data obtained in this investigation from the location of $M = 1$ on the shock wave, the separation distance of the shock wave, and the sonic line joining the cone at the corner as indicated from the pressure data. No information can be offered as to the shape of the sonic line joining the cone and the shock wave.

c. Blocking tests.

The results of this section would have been of assistance in setting up this test program as it gives a good indication of the size of cylindrical models that can be tested in this wind tunnel. From inspection of Fig. 62, it can be seen that while the tunnel is unblocked, the cone size has reached the upper limit that would be

practical due to the considerations of disturbed flow. The shape of the $\Delta A/A$ curve in Fig. 64, is very similar to the one-dimensional predicted curve except that it is merely shifted due to boundary layer.

REFERENCES

1. Puckett, Allen E. and Schamberg, Richard, "Final Report - Galcit Supersonic Wind Tunnel Tests", Library of Aeronautics, California Institute of Technology, June, 1946.

2. Puckett, Allen E., "Supersonic Nozzle Design", Journal of Applied Mechanics, December, 1946.

3. Kopal, Z., "Supersonic Flow Around Cones", M.I.T. Center of Analysis, Report No. 1.

4. Maccell, J. W. and Codd, J., Theoretical Research Report No. 17/45, September, 1945.

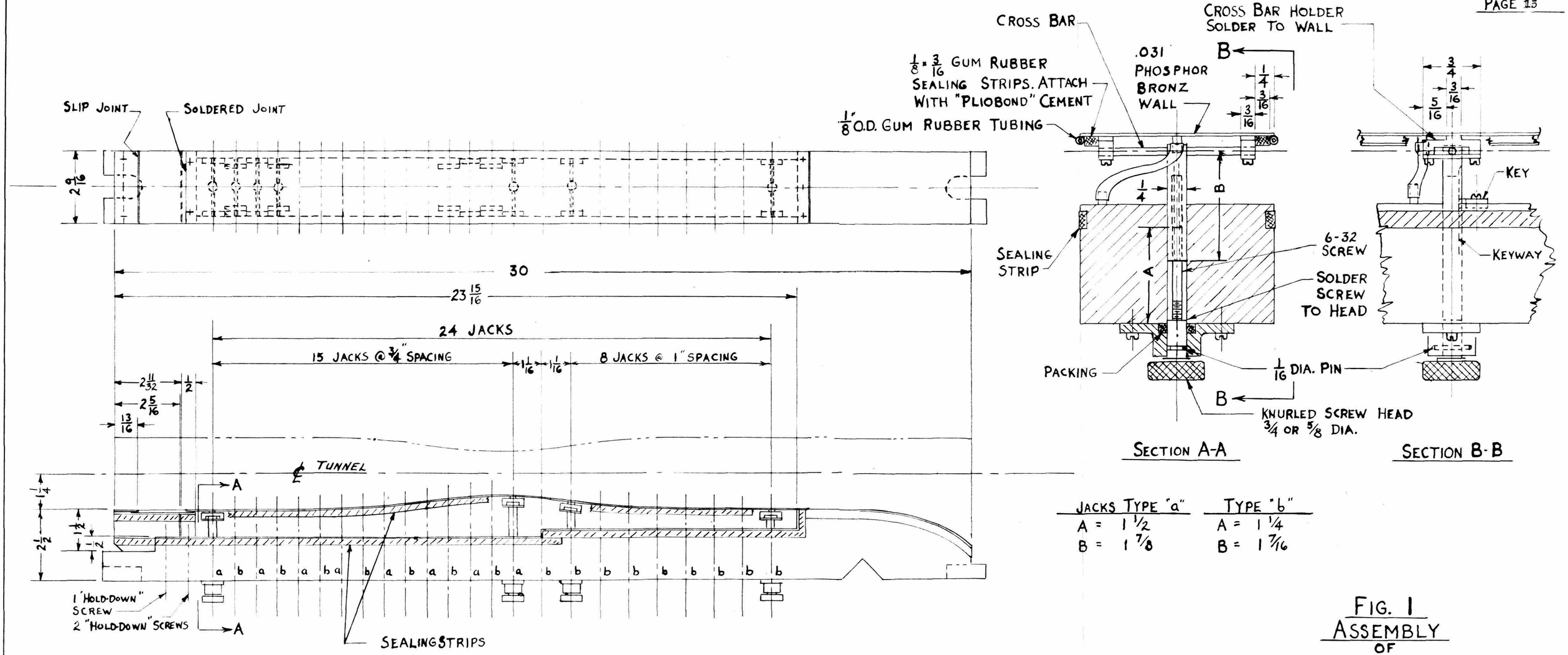

SECTION A-A

SECTION B-B

JACKS	TYPE "a"	TYPE "b"
A =	1 1/2	1 1/4
B =	1 7/8	1 7/16

FIG. 1
ASSEMBLY OF FLEXIBLE NOZZLE BLOCKS

J.H.G. 5-20-48

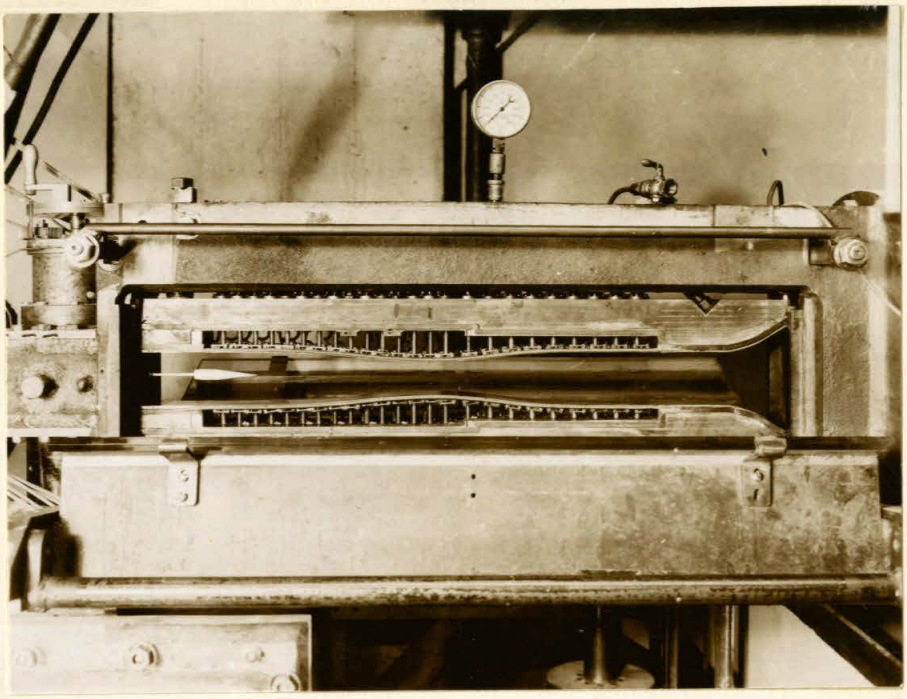

Fig. 2

General View of the Flexible Nozzle

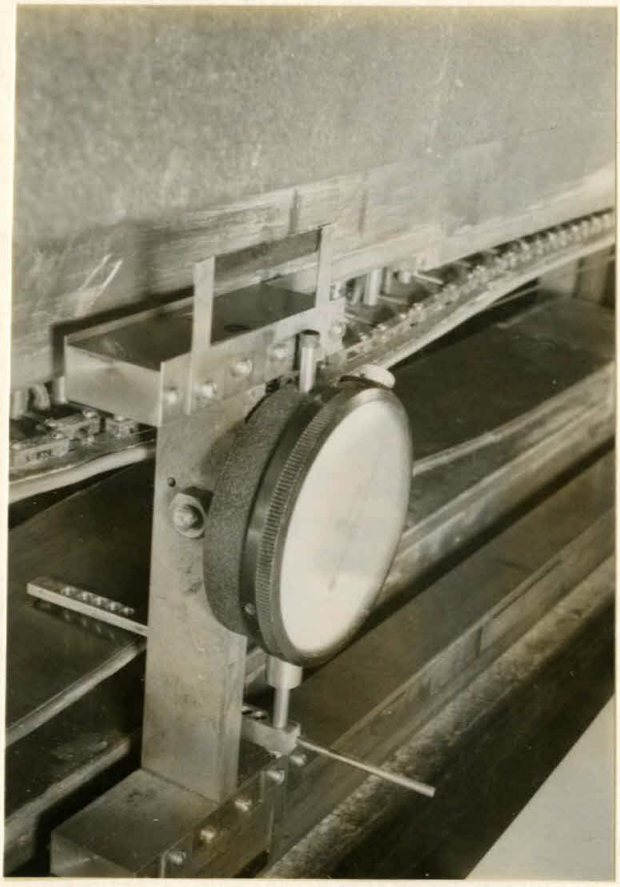

Fig. 3

View of the Calibration Set Up

FIG. 4 CENTER LINE SURVEY M= 1.58

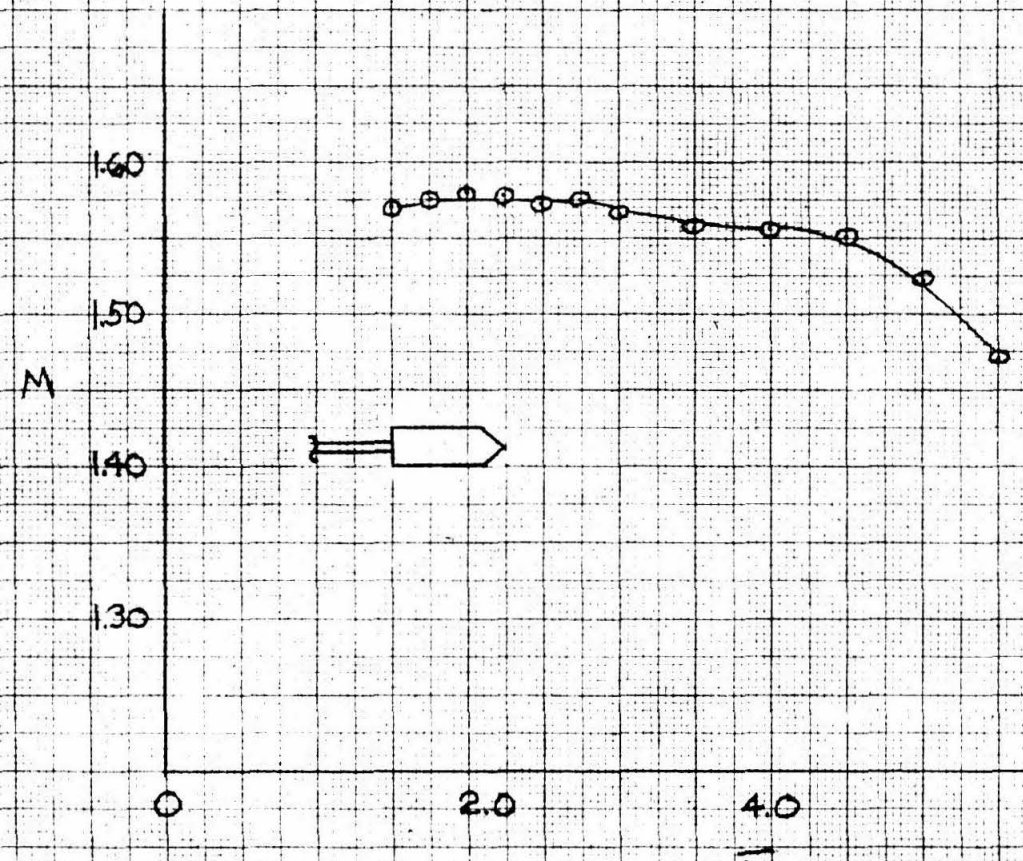

FIG. 5
CONE PRESSURE MODELS

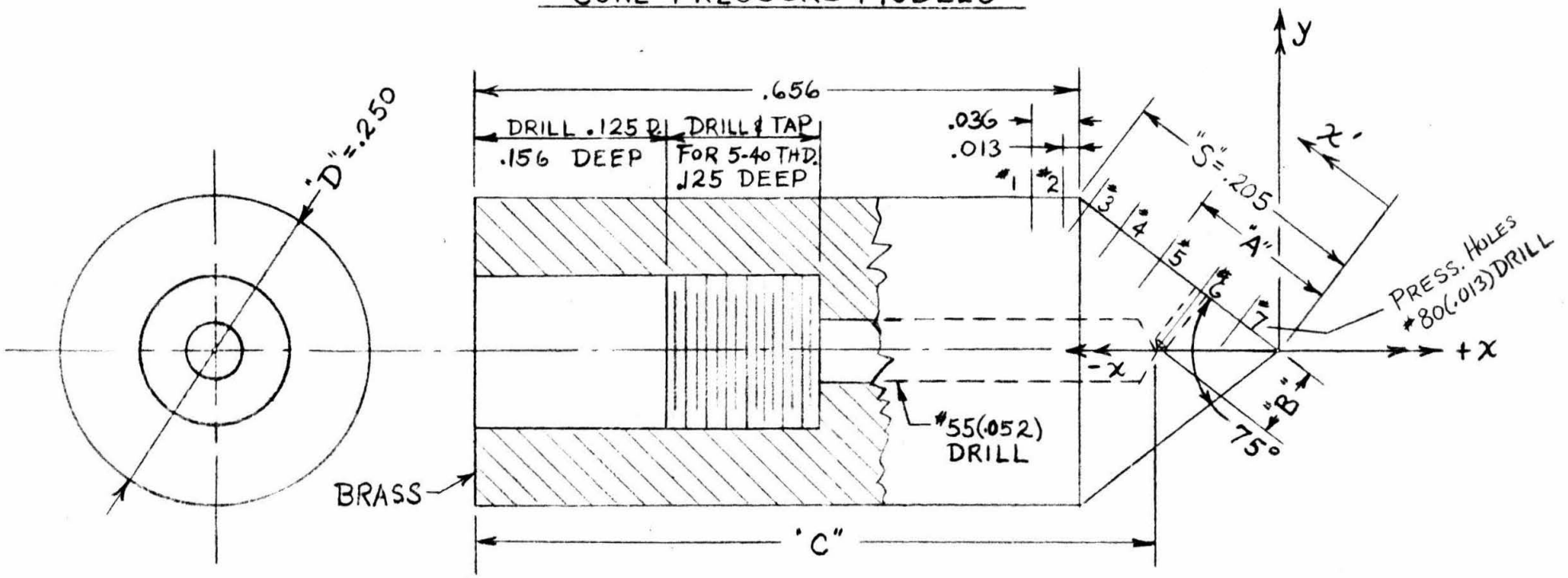

* DRILL ONE PRESSURE PER CONE. I.E. CONE #1 HAS HOLE #1, ETC.

CONE NO.*	"A" (INCH) NOMINAL	"A" (INCH) ACTUAL	"B" (INCHES)	"C" (INCHES)
1			.125	.656
2			.125	.656
3	.195	.197	.130	.656
4	.164	.159	.130	.666
5	.123	.122	.100	.712
6	.082	.078	.065	.750
7	.041	.042	.060	.773

FIG. 6 : 75° CONE PRESSURE DISTRIBUTION

$M_1 = 1.41$

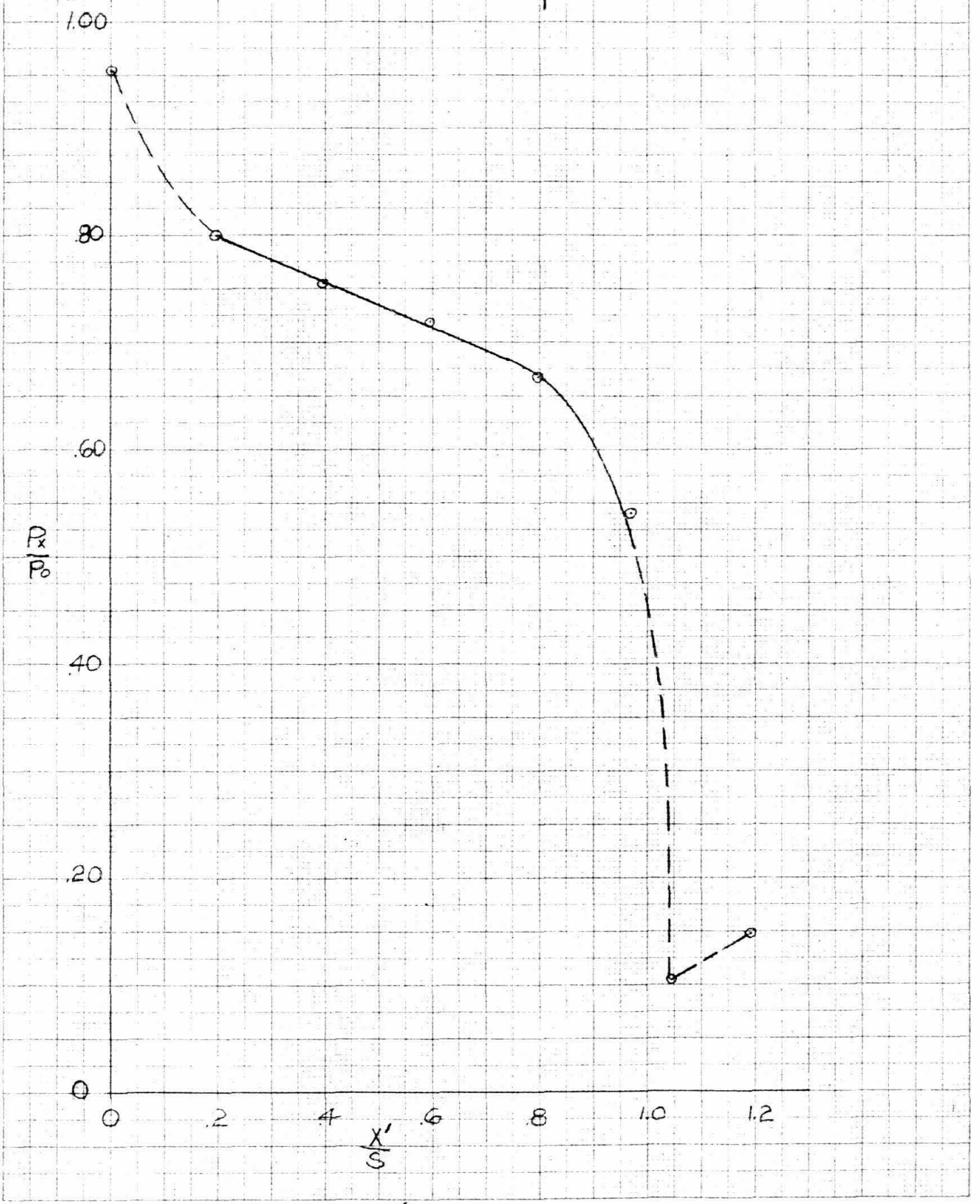

FIG. 7: 75° CONE PRESSURE DISTRIBUTION

$M_1 = 1.490$

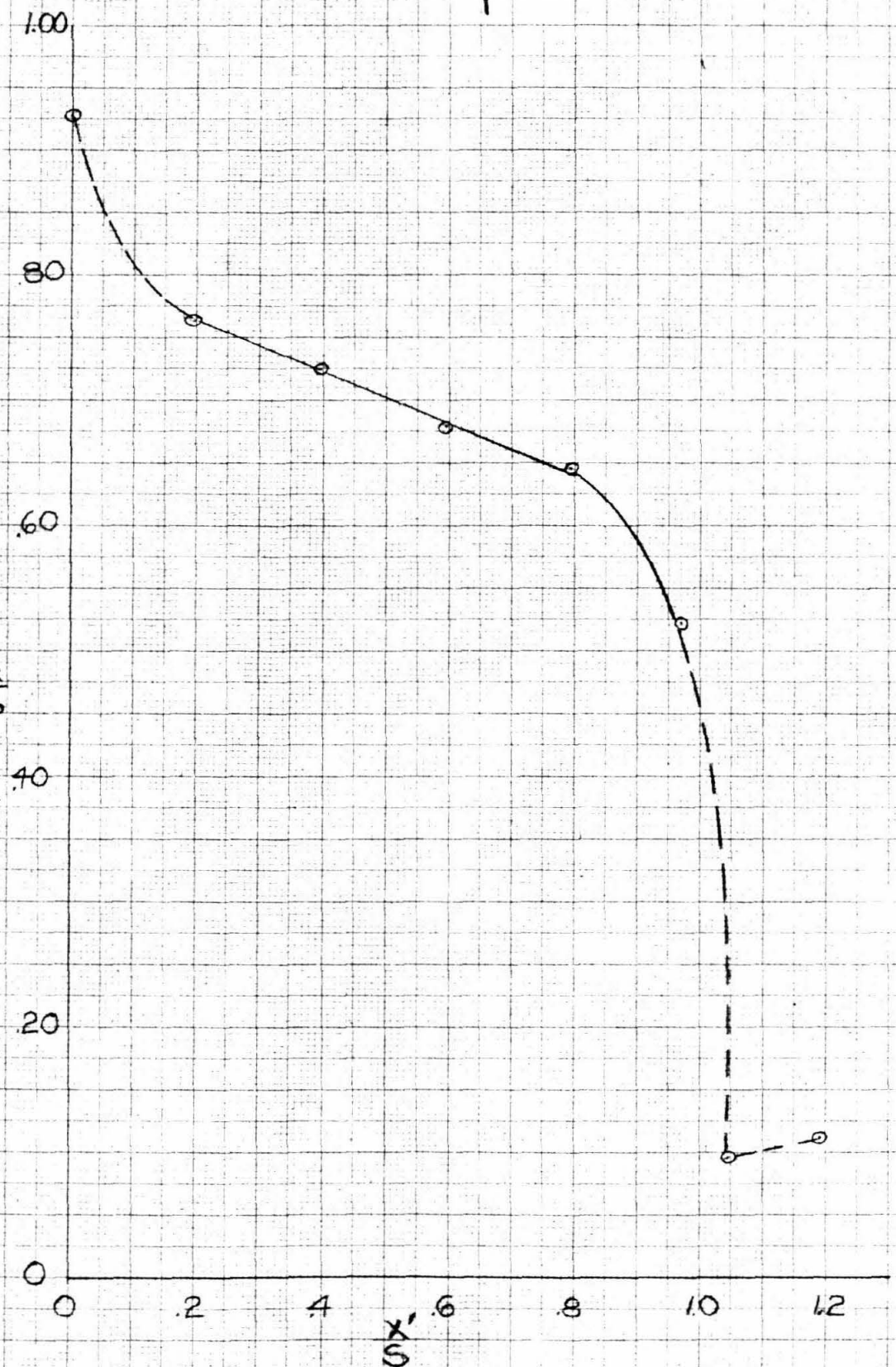

FIG. 8 75° CONE PRESSURE DISTRIBUTION
$M_1 = 1.58$

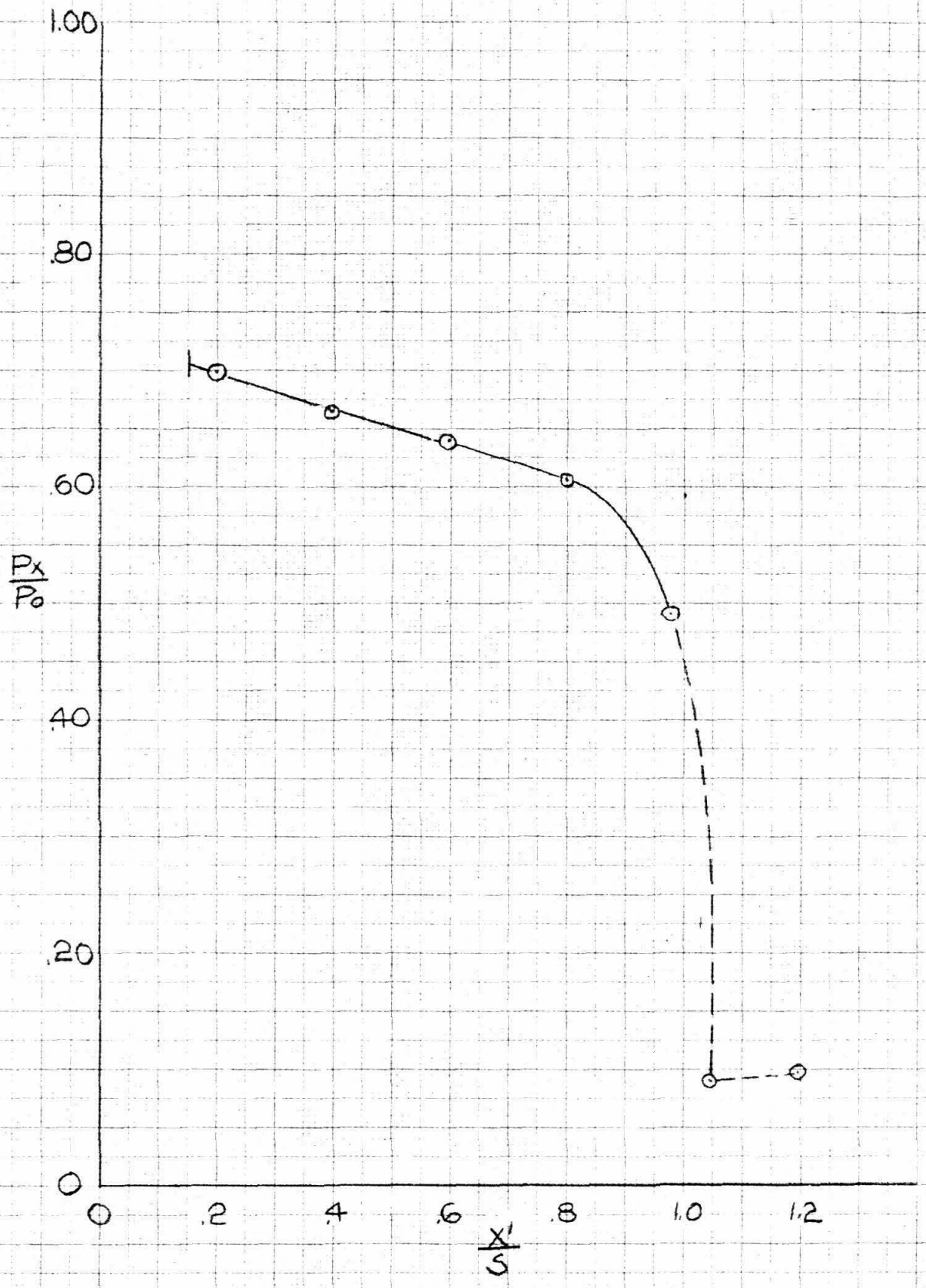

FIG. 9 75° CONE PRESSURE DISTRIBUTION
$M_1 = 1.71$

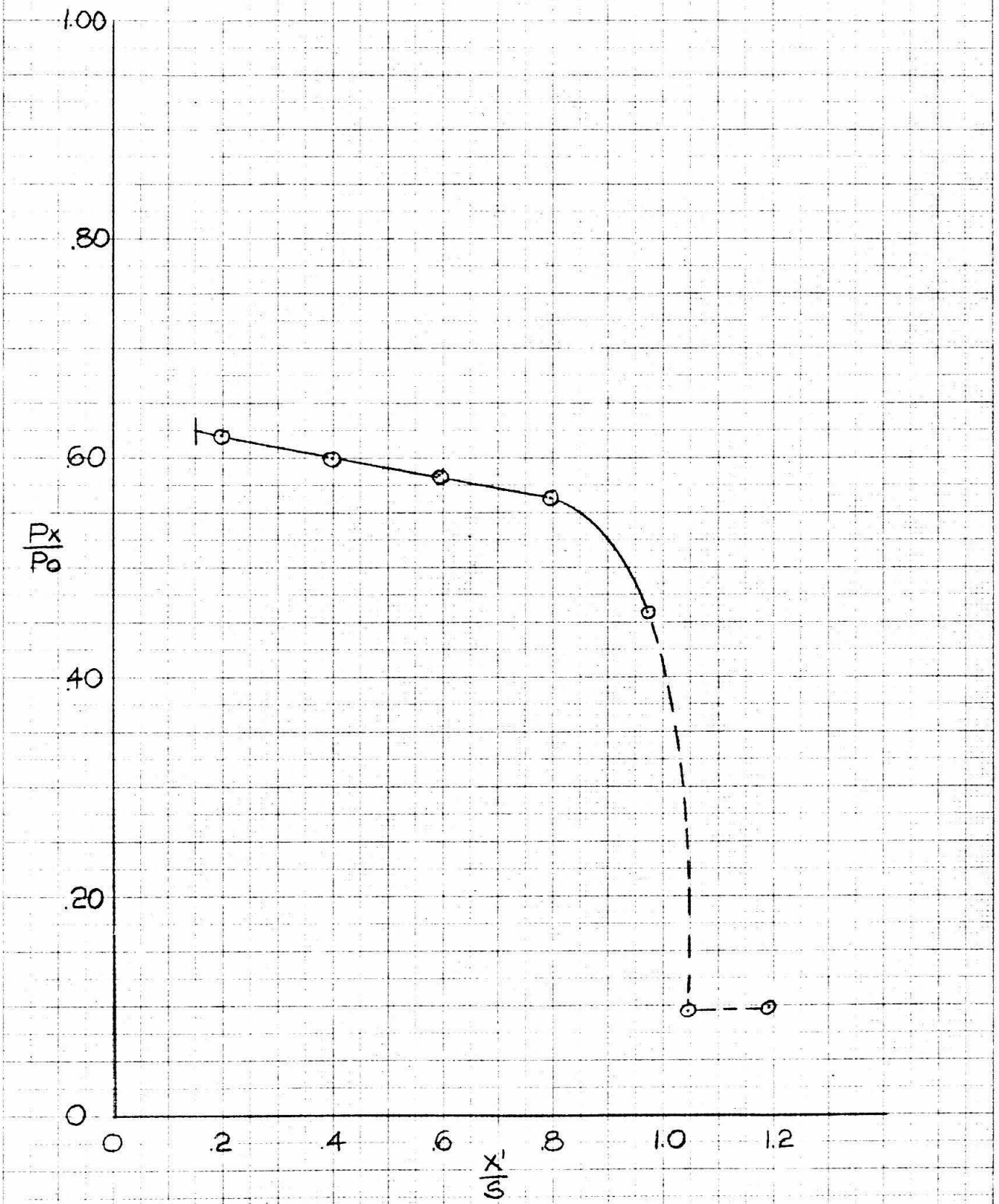

FIG. 10 75° CONE PRESSURE DISTRIBUTION

$M_1 = 1.83$

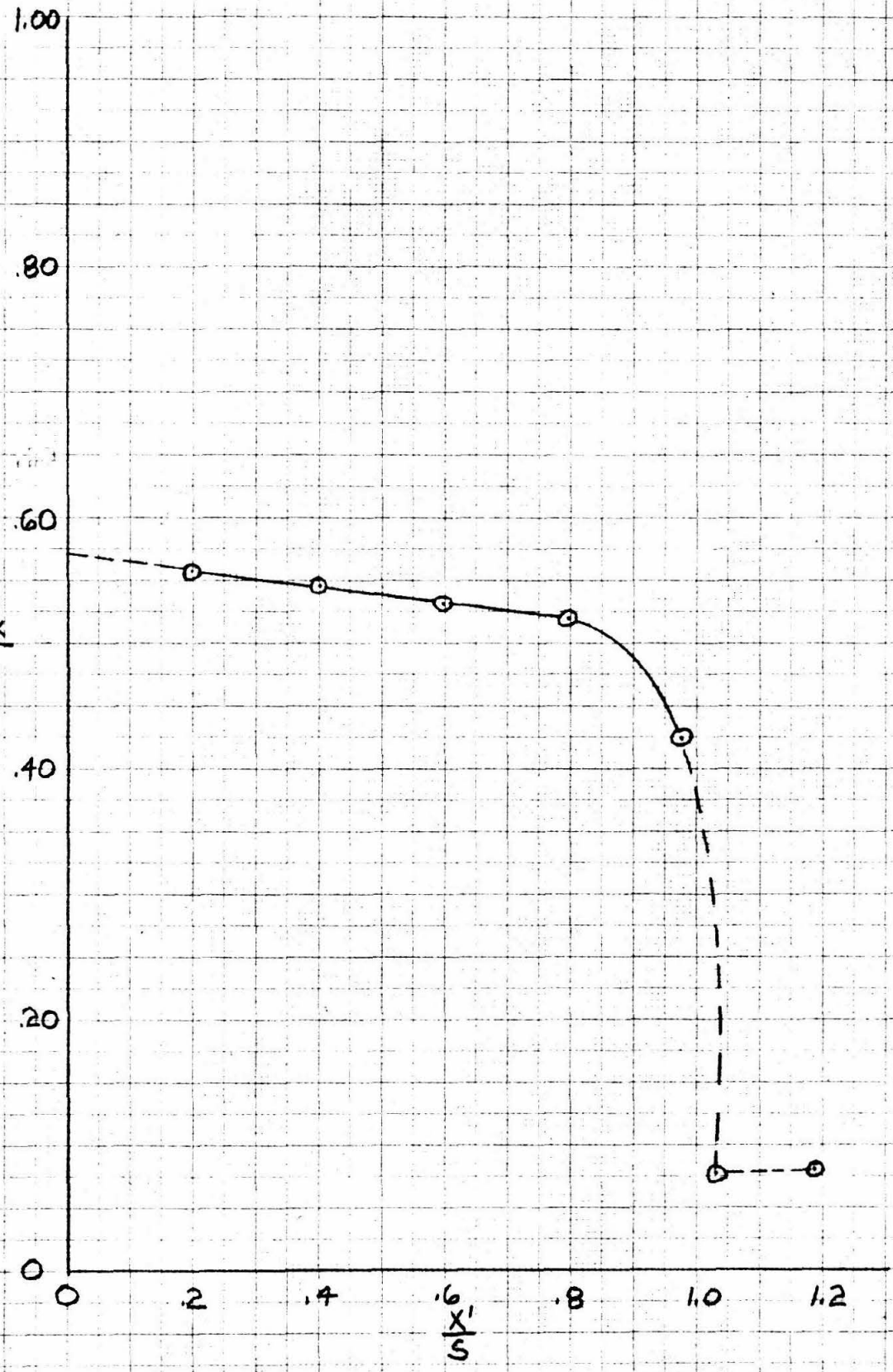

FIG. 11 75° CONE PRESSURE DISTRIBUTION

$M_1 = 1.99$

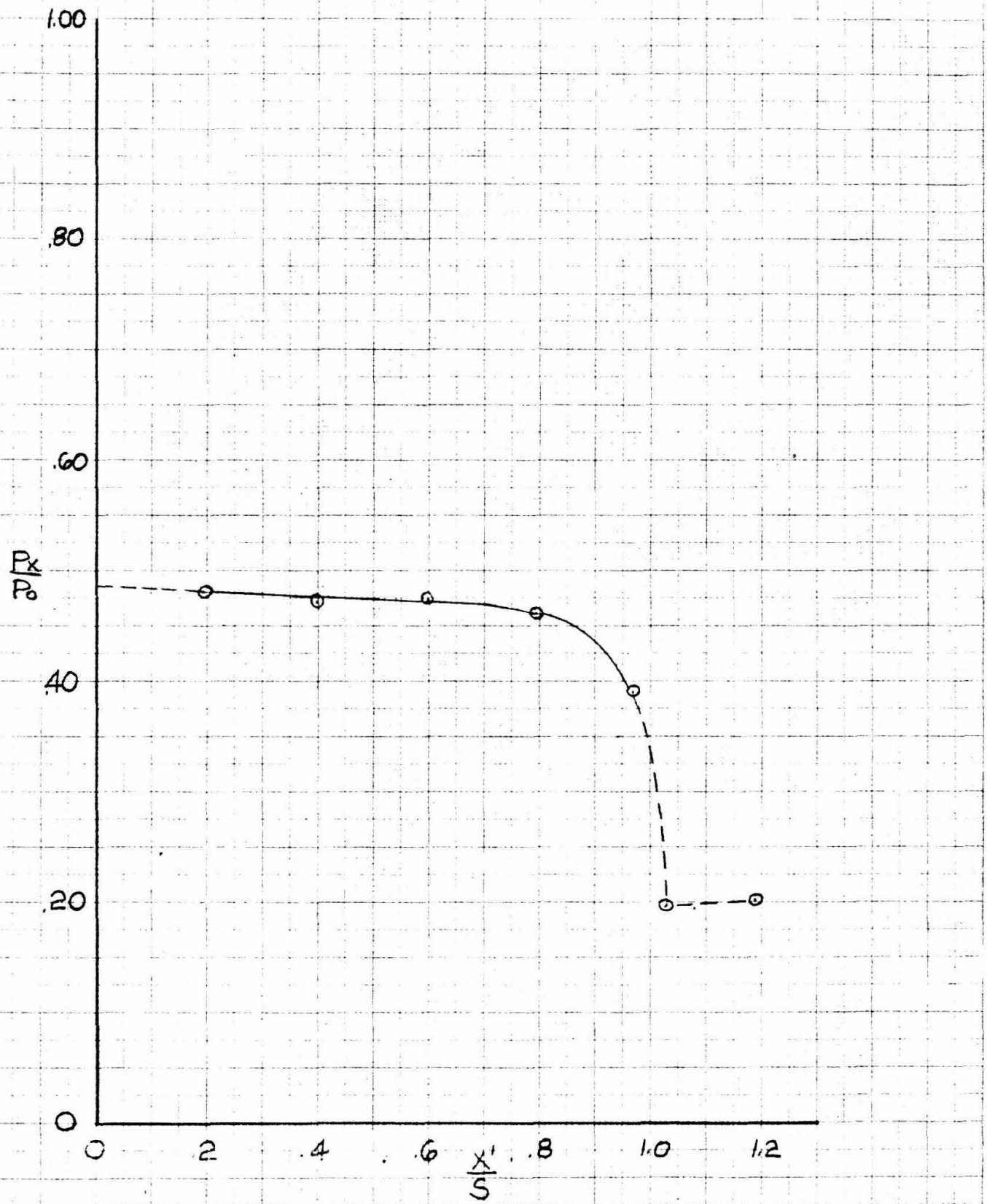

FIG 12 75° CONE PRESSURE DISTRIBUTION

SUMMARY

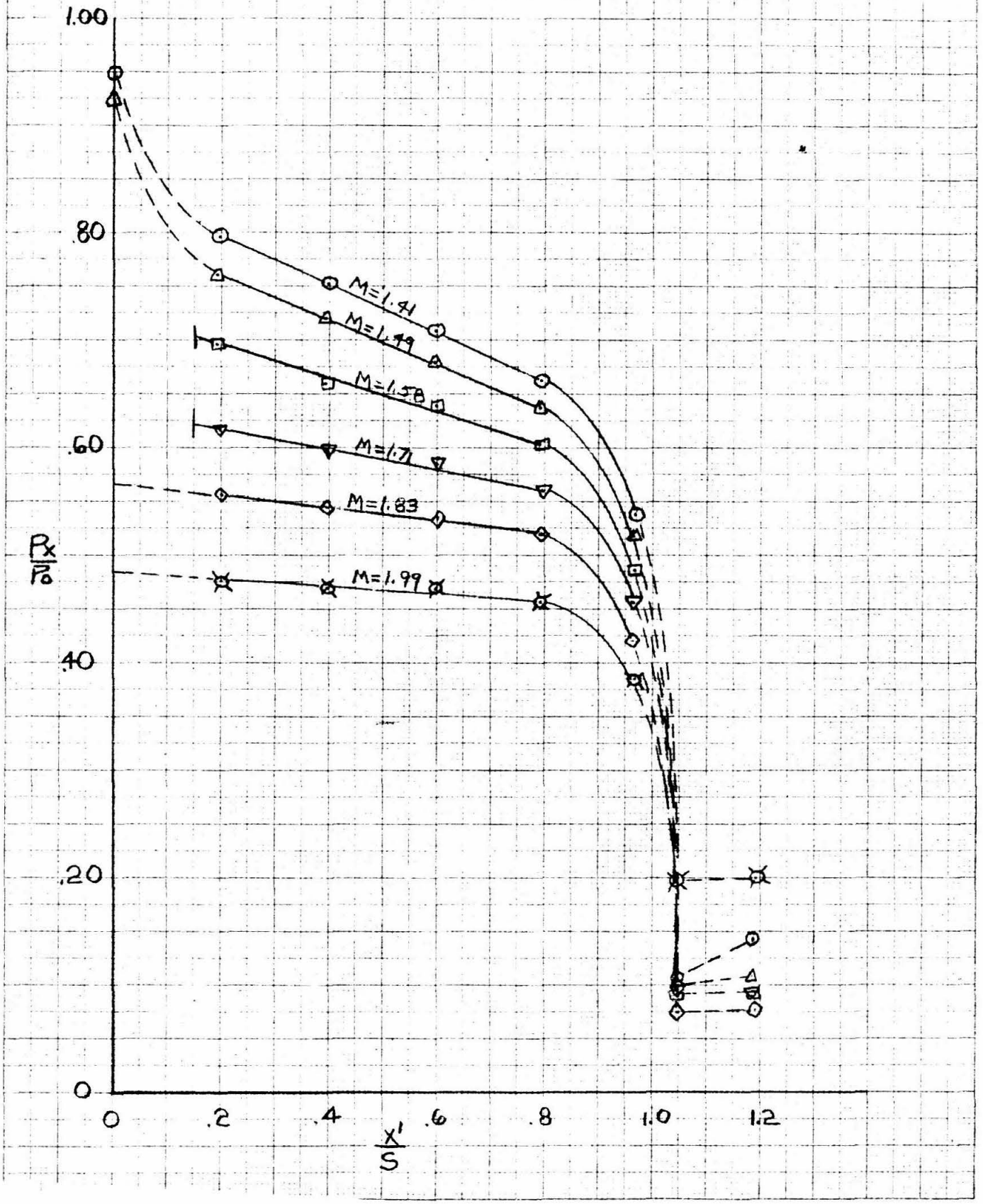

FIG. 13: 75° CONE PRESSURE DISTRIBUTION

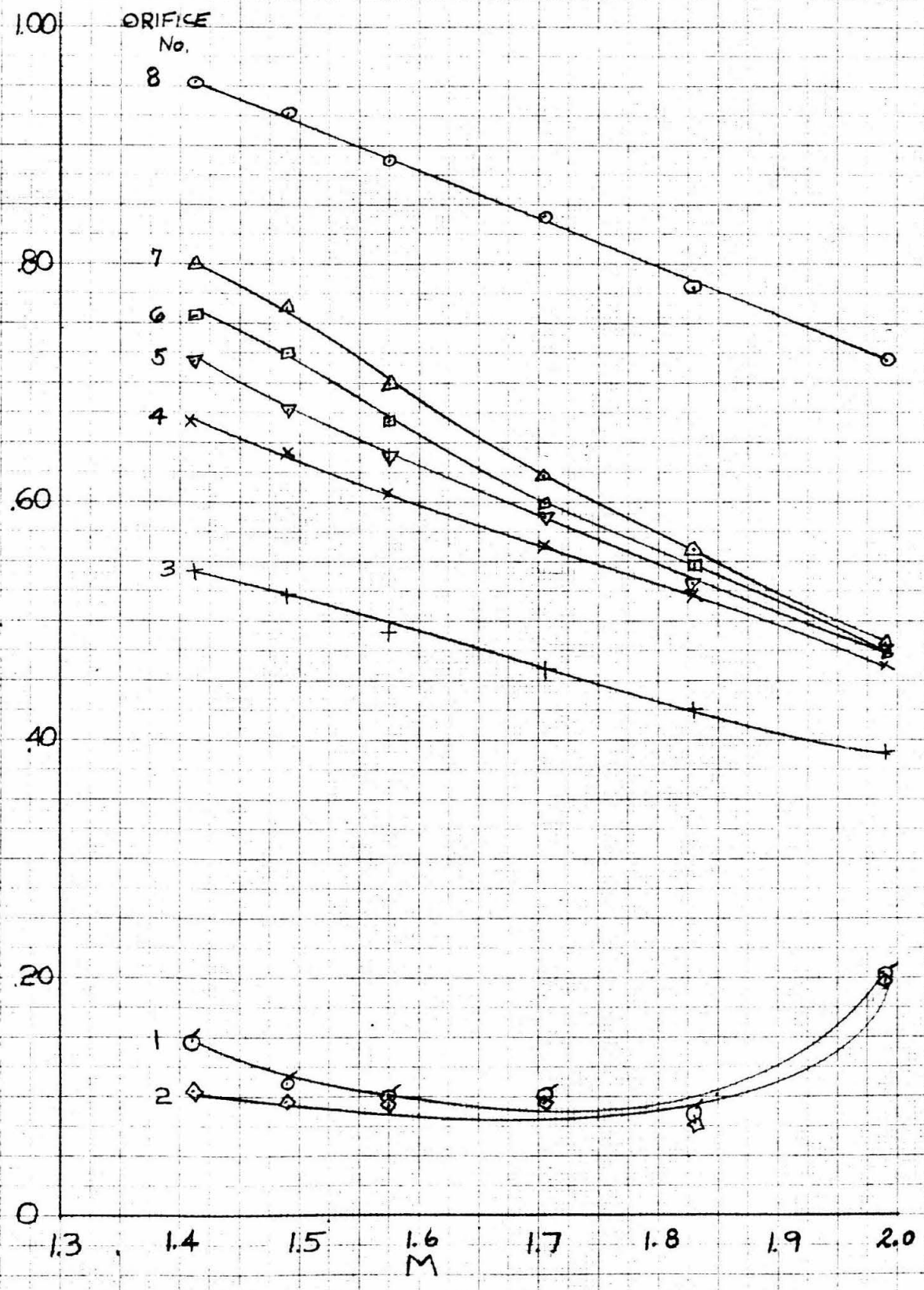

FIG. 14: 75° CONE PRESSURE DISTRIBUTION
$M_1 = 1.41$

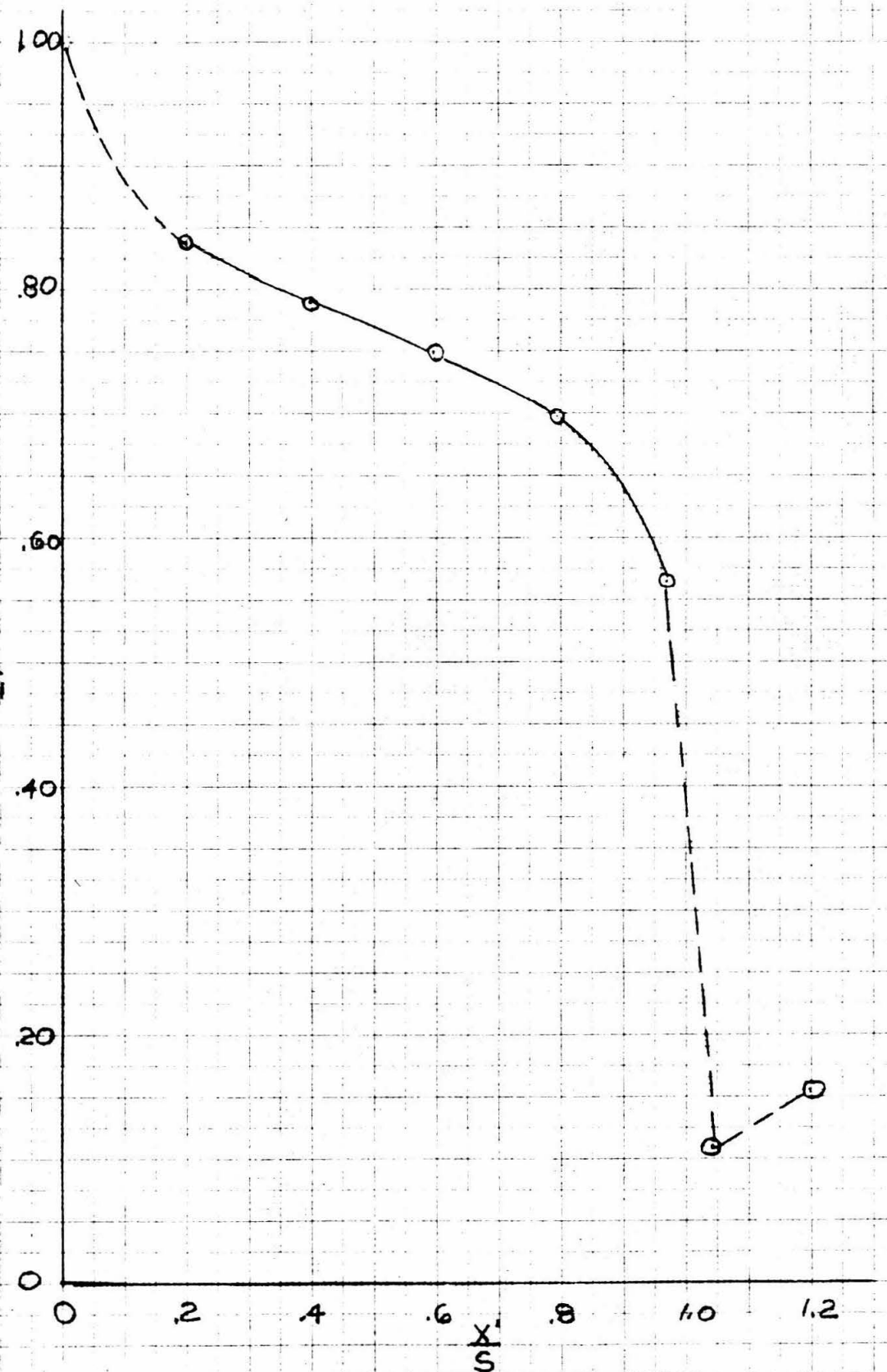

FIG. 15: 75° CONE PRESSURE DISTRIBUTION
$M_1 = 1.49$

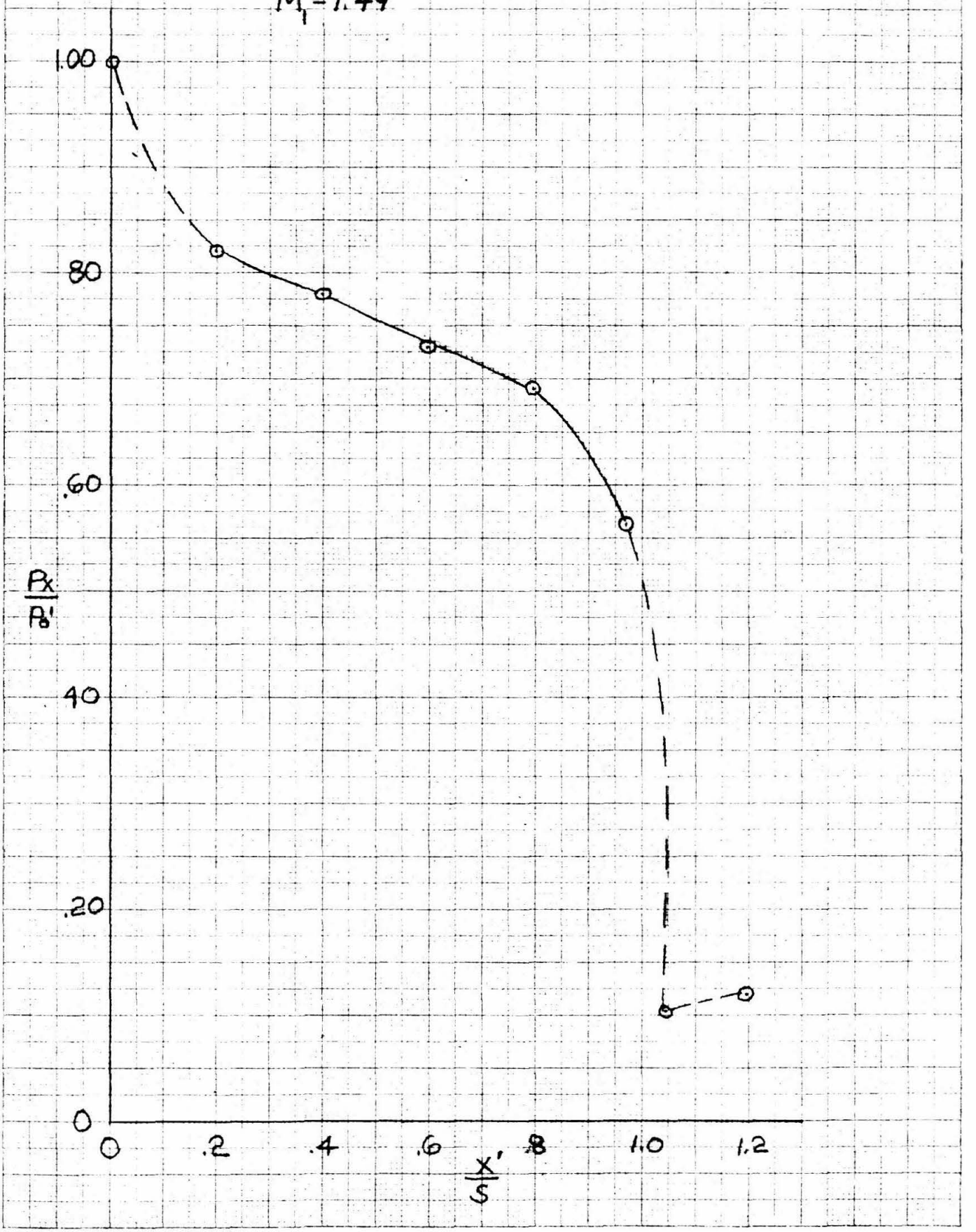

FIG. 16 75° CONE PRESSURE DISTRIBUTION
$M_1 = 1.58$

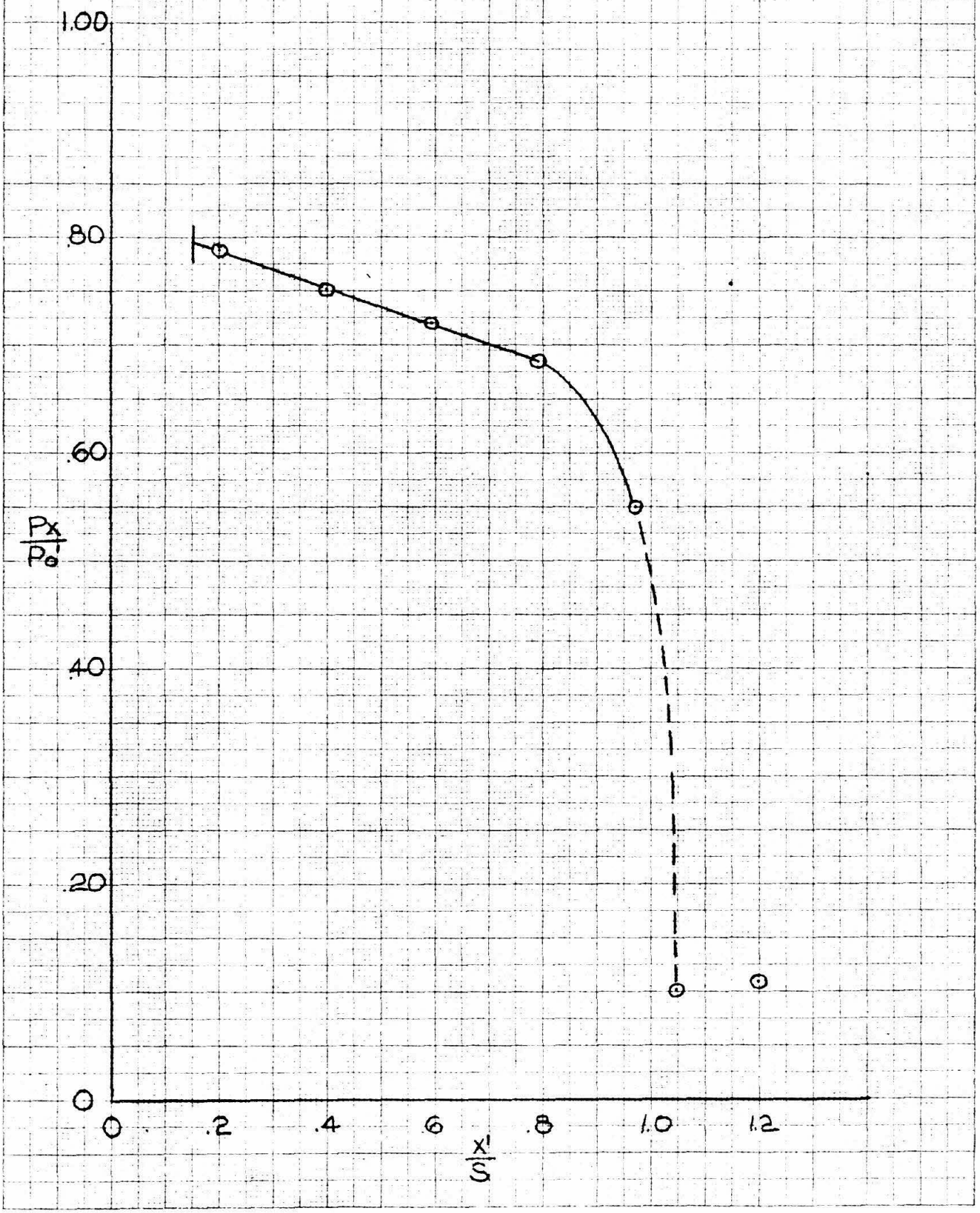

FIG. 17 75° CONE PRESSURE DISTRIBUTION
$M_1 = 1.71$

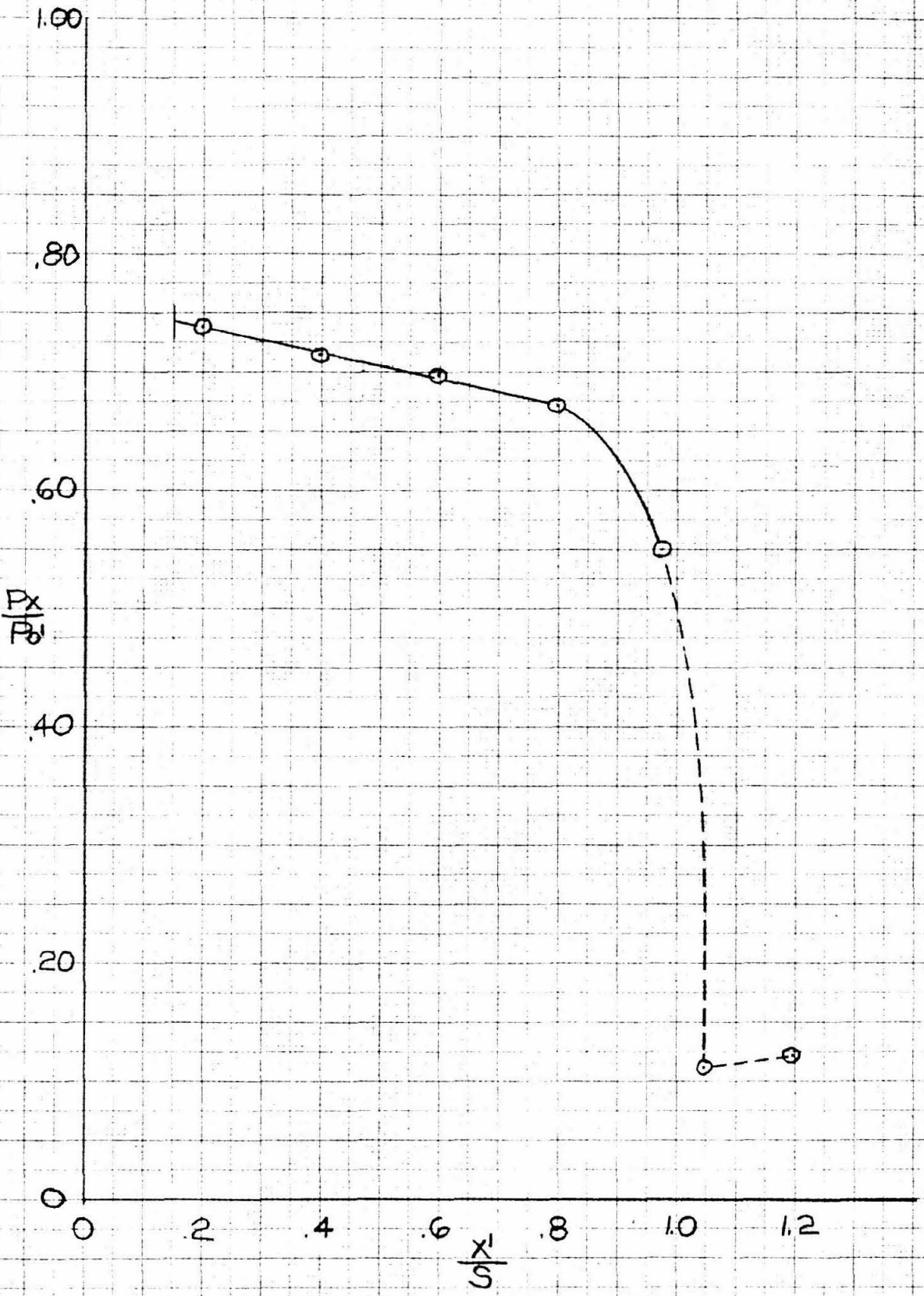

FIG. 18 75° CONE PRESSURE DISTRIBUTION

$M_1 = 1.83$

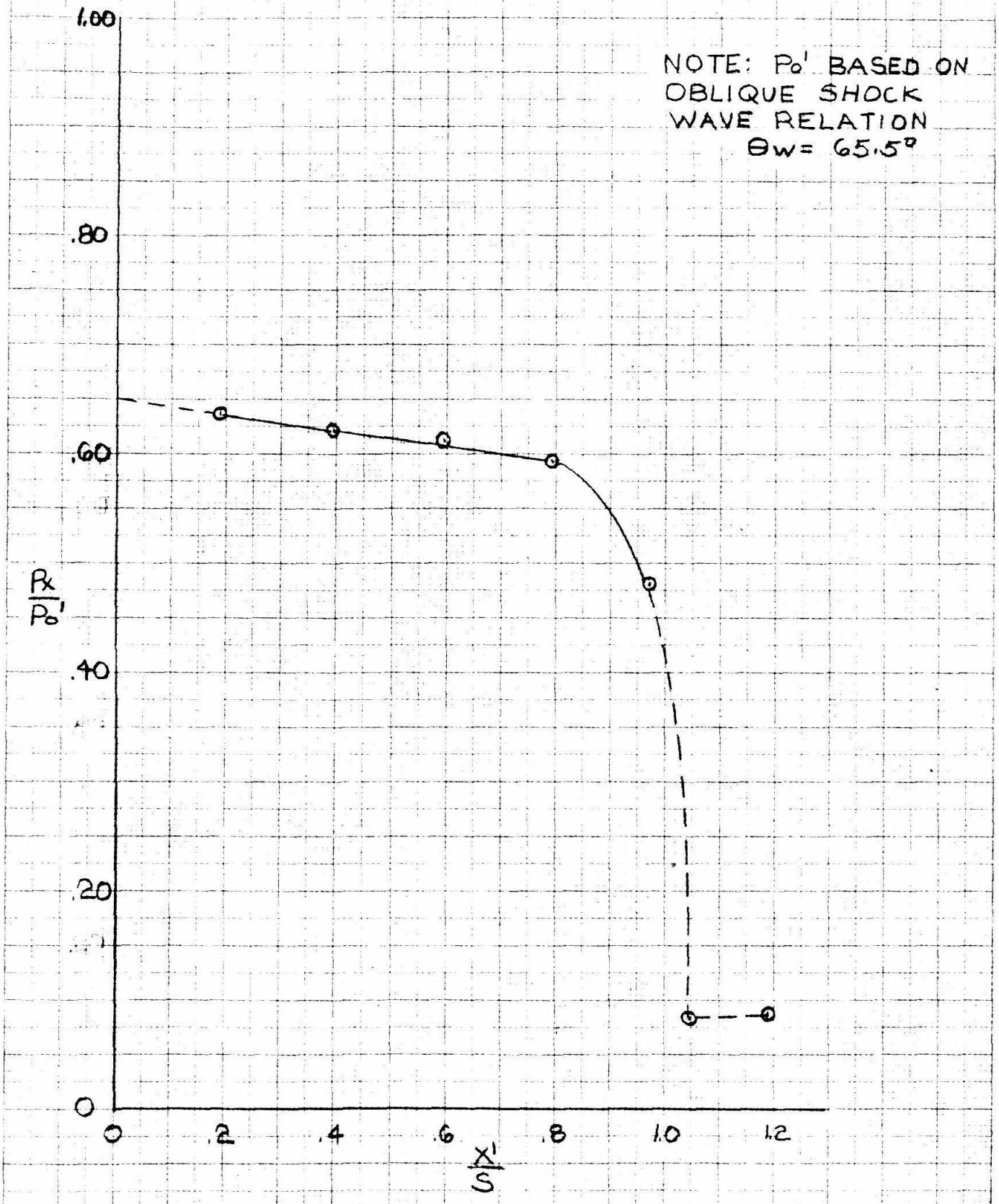

FIG. 19 75° CONE PRESSURE DISTRIBUTION

$M_1 = 1.99$

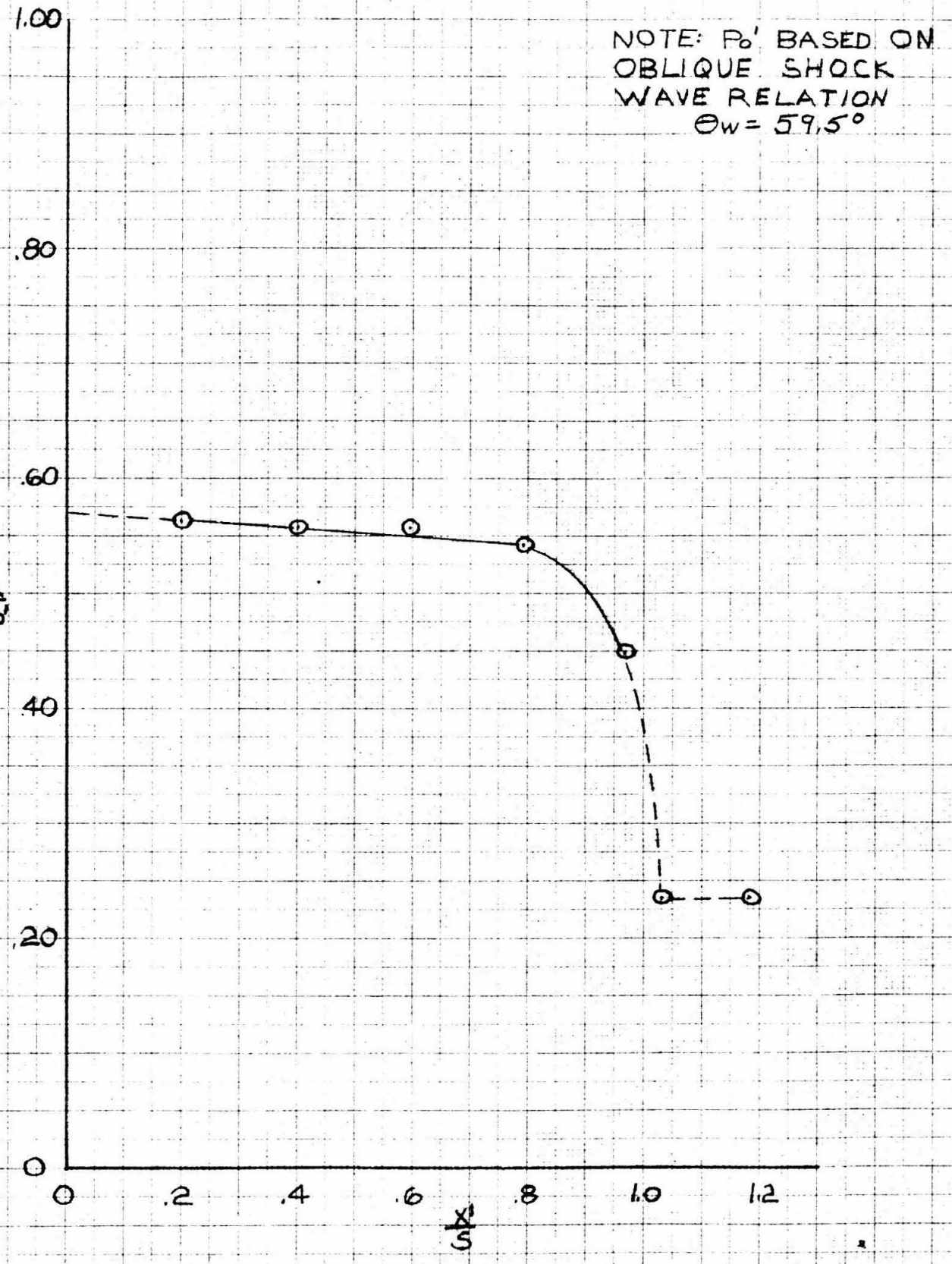

FIG 20 75° CONE PRESSURE DISTRIBUTION SUMMARY

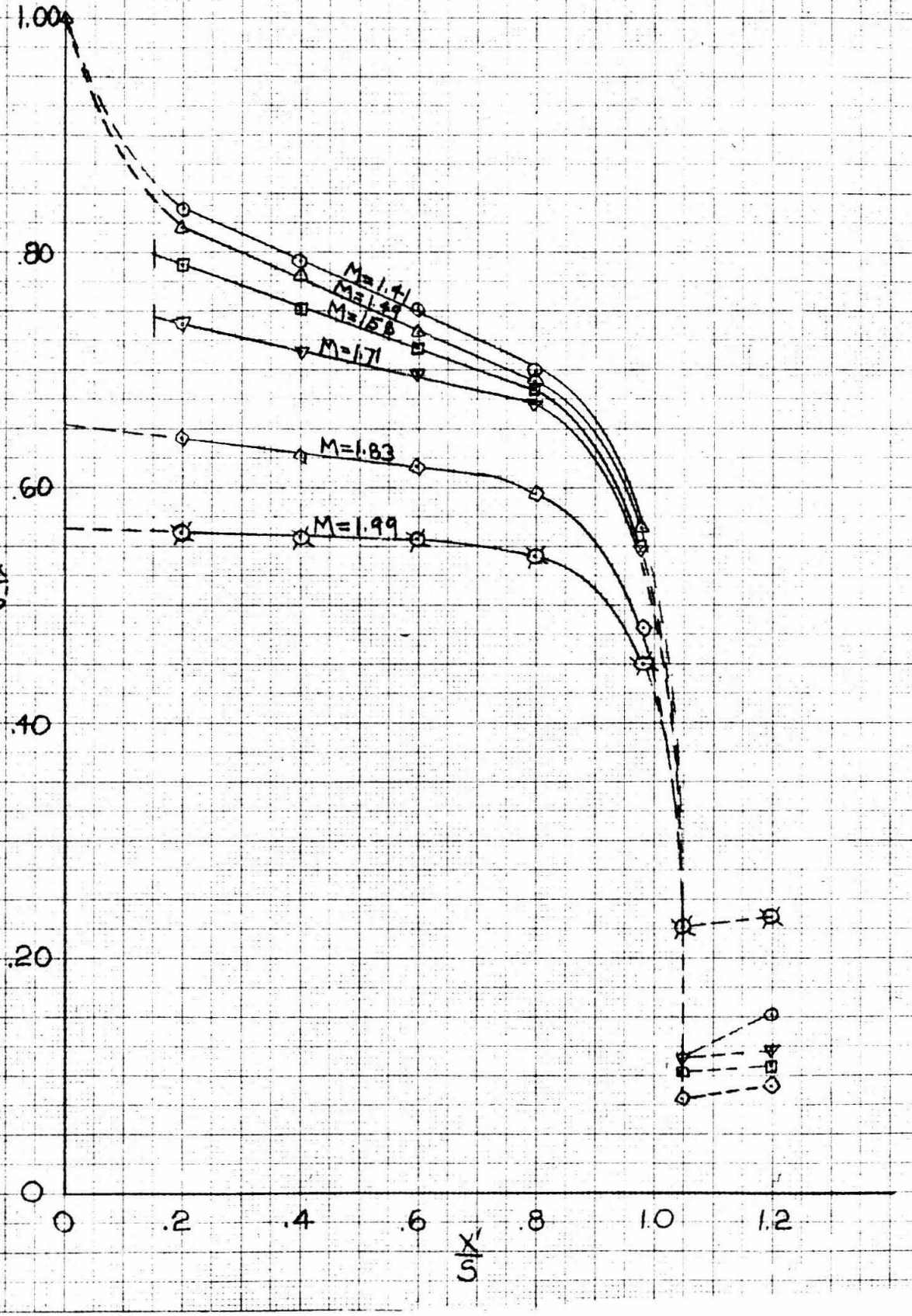

FIG. 21 75° CONE PRESSURE DISTRIBUTION

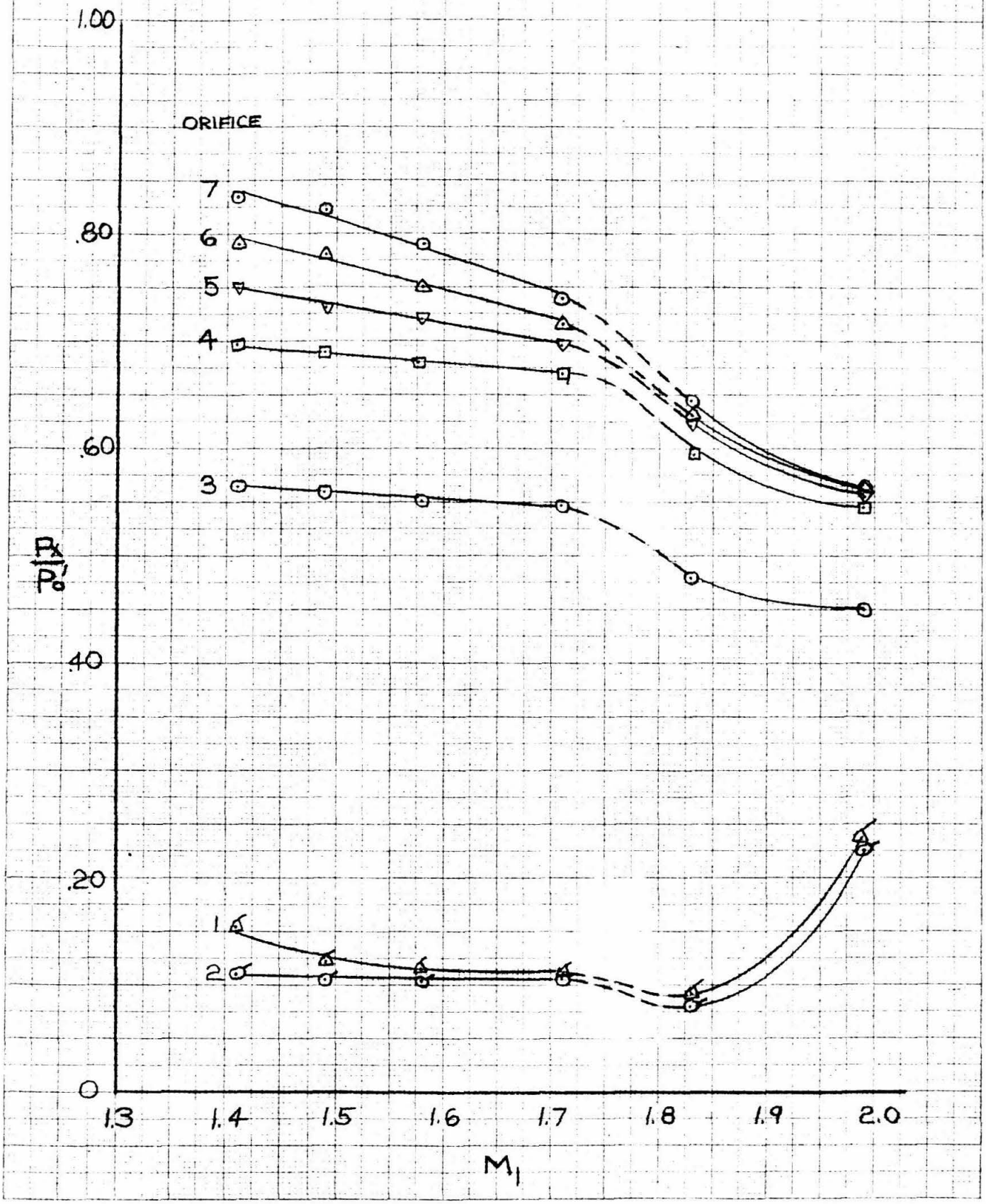

FIG. 22

COMPARISON
TOTAL HEAD RATIOS
CALCULATED VS. BLUNT CYLINDER

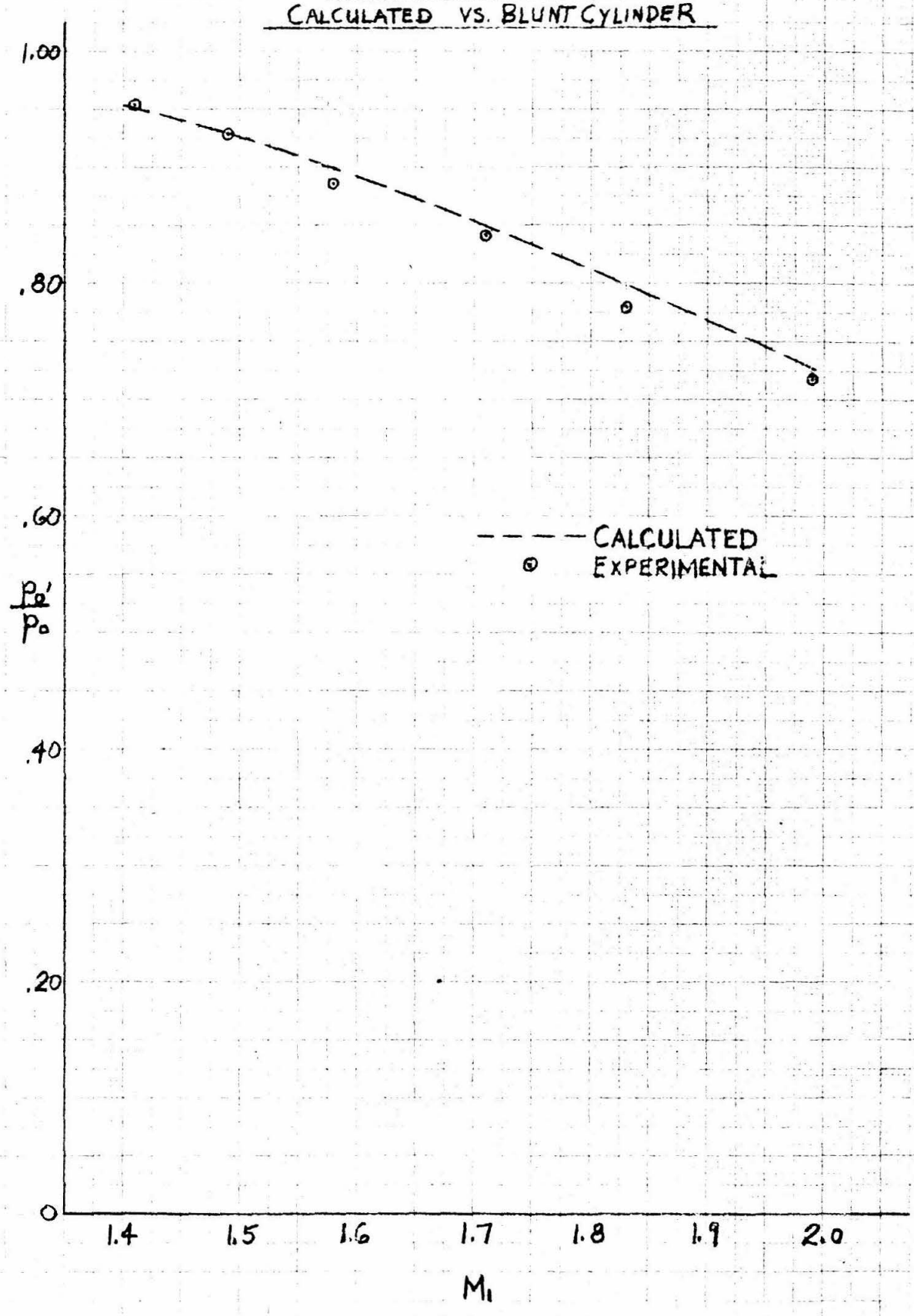

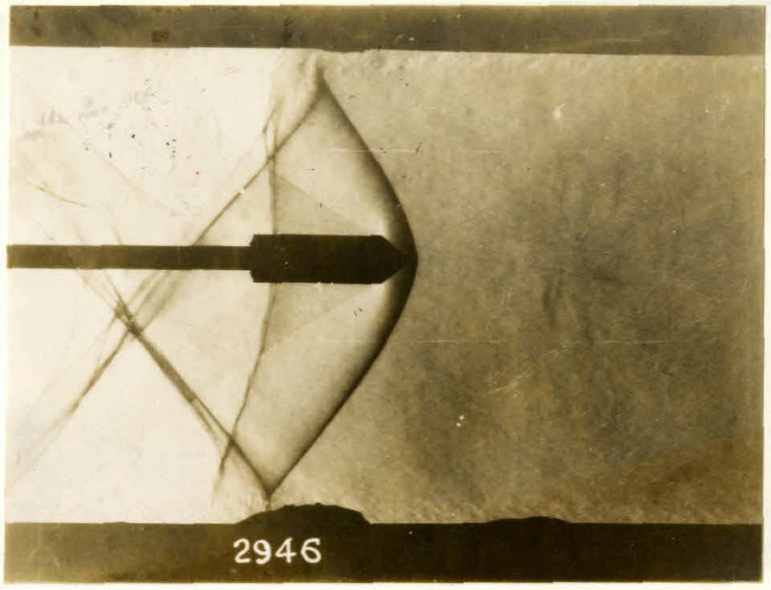

Fig. 23

75° Cone, M = 1.41

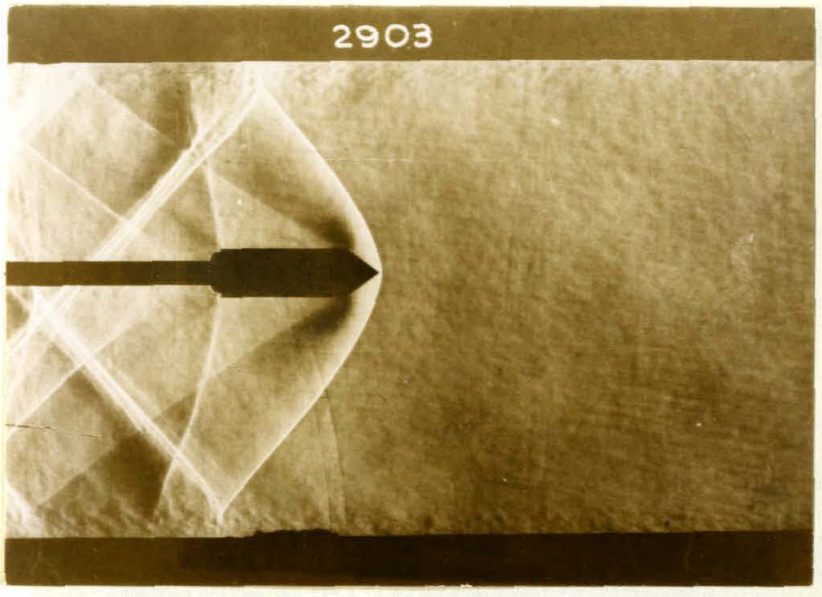

Fig. 24

75° Cone, M = 1.49

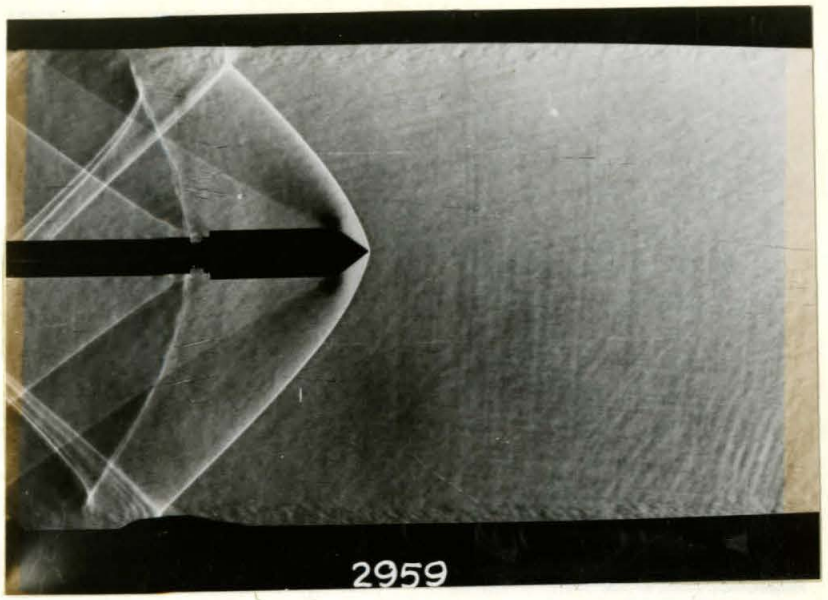

Fig. 25

75° Cone, M = 1.58

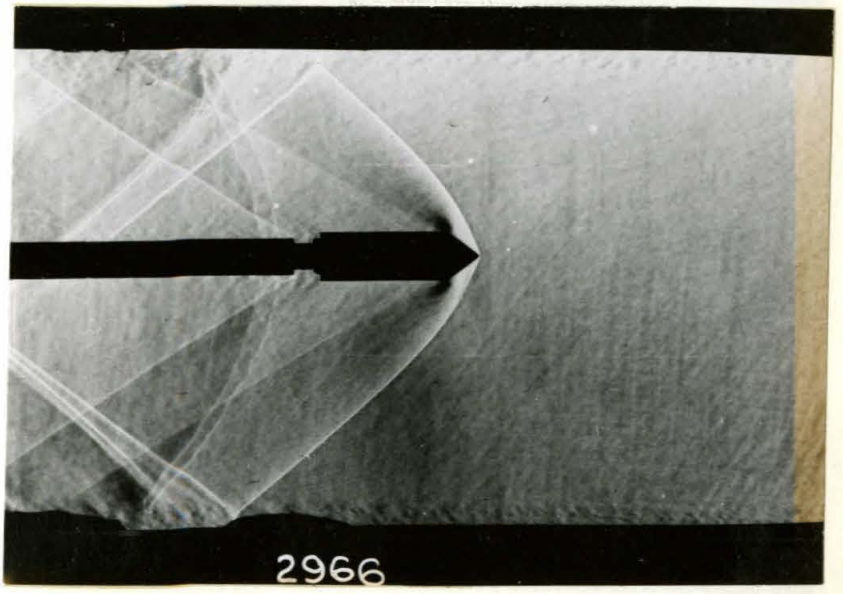

Fig. 26

75° Cone, M = 1.71

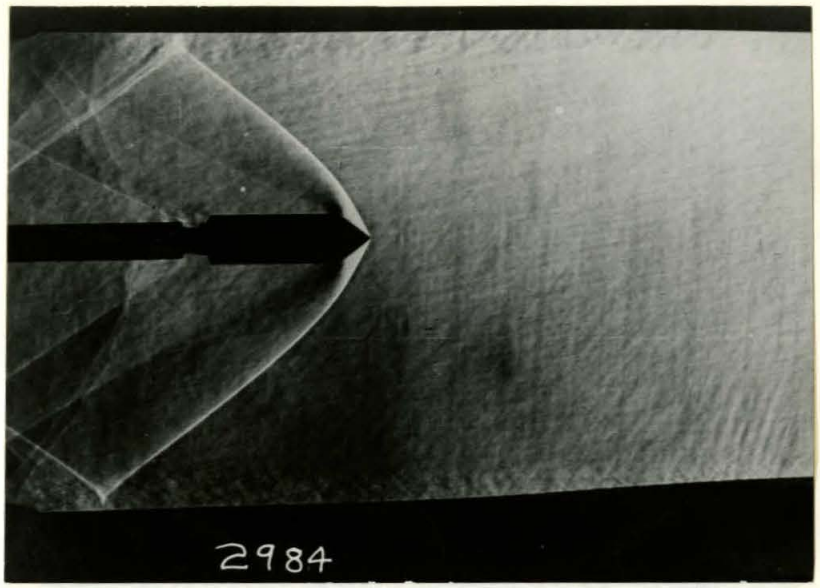

Fig. 27

75° Cone, M = 1.83

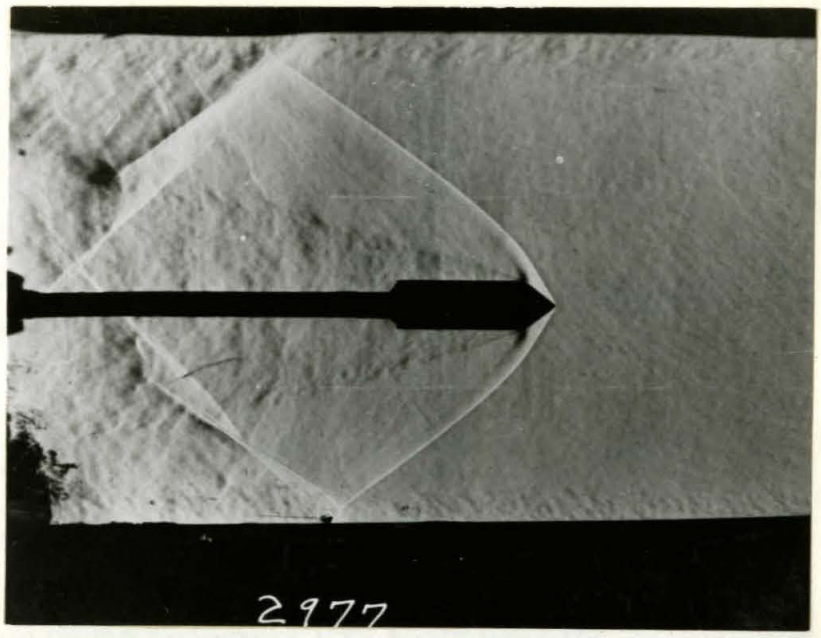

Fig. 28

75° Cone, M = 1.99

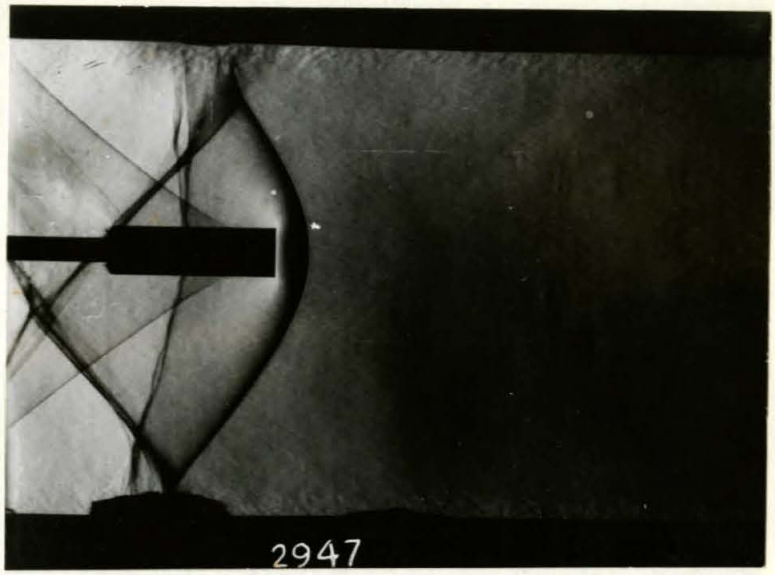

Fig. 29

Blunt Cylinder, M = 1.41

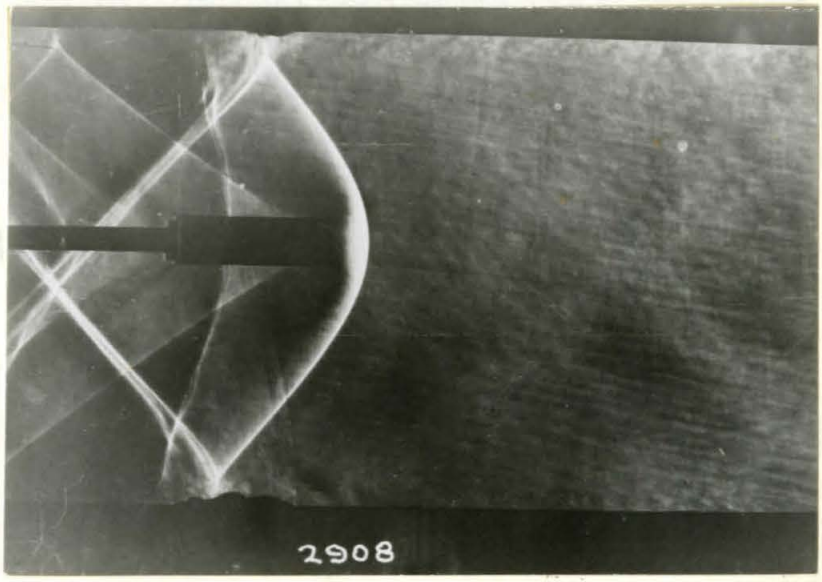

Fig. 30

Blunt Cylinder, M = 1.49

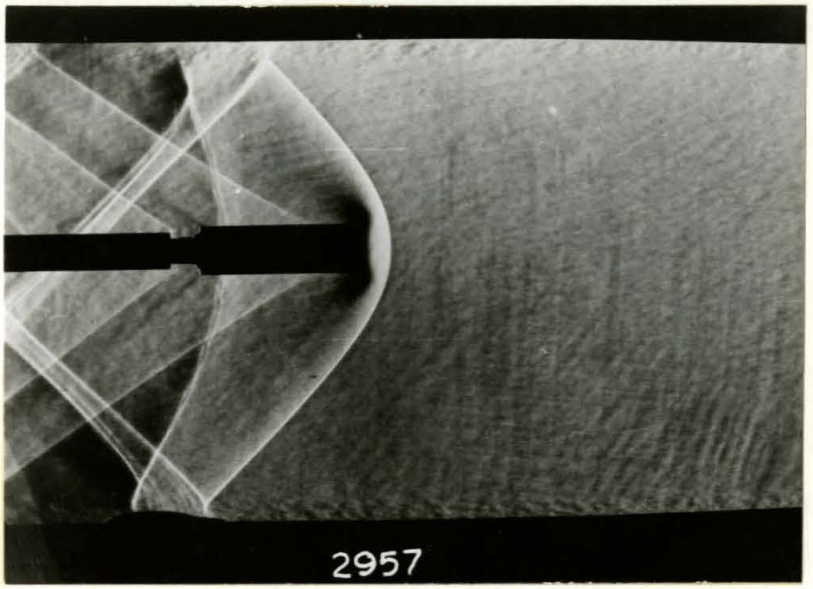

Fig. 31

Blunt Cylinder, M = 1.58

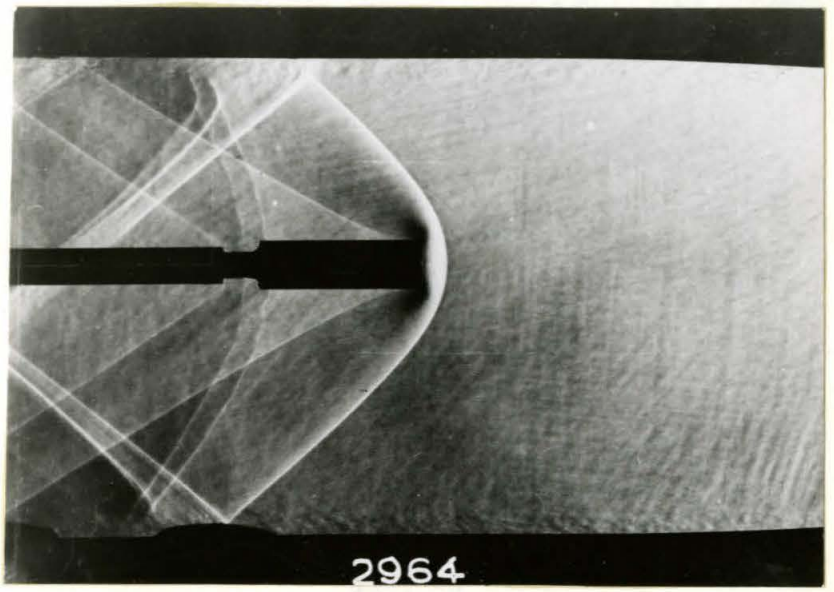

Fig. 32

Blunt Cylinder, M = 1.71

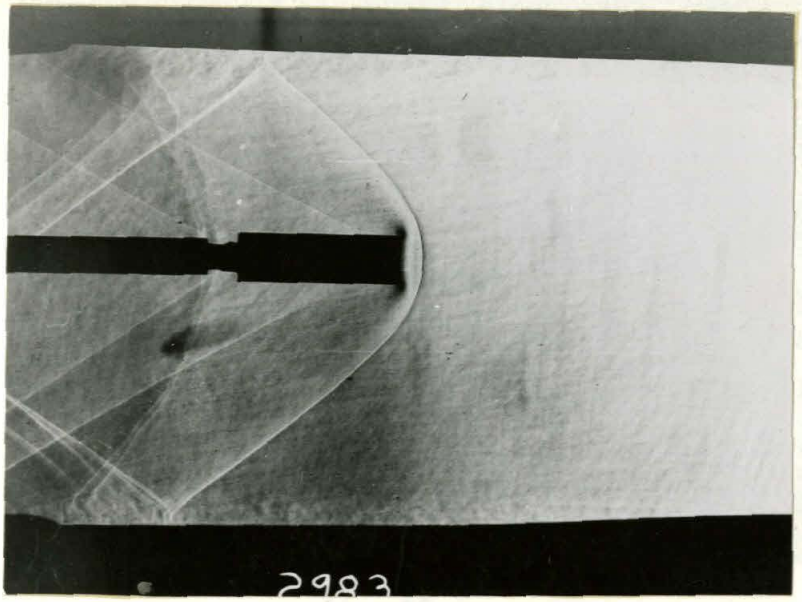

Fig. 33

Blunt Cylinder, M = 1.83

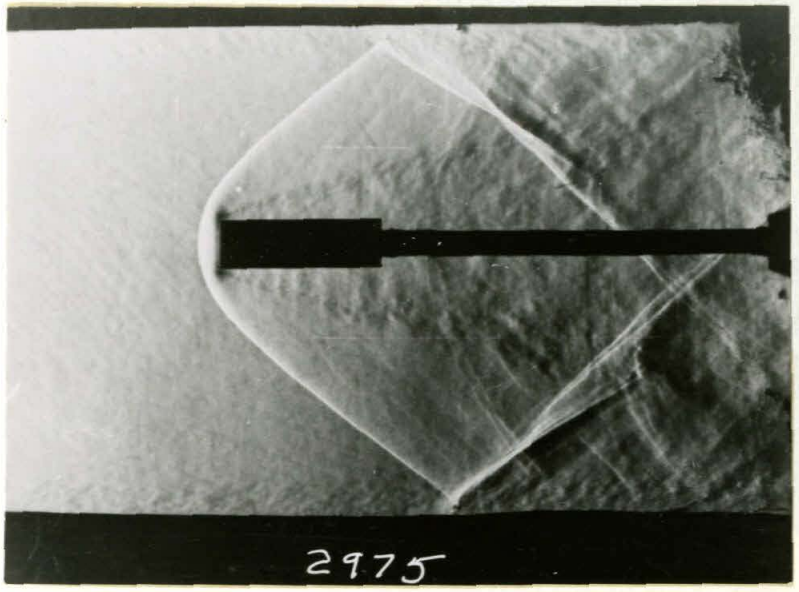

Fig. 34

Blunt Cylinder, M = 1.99

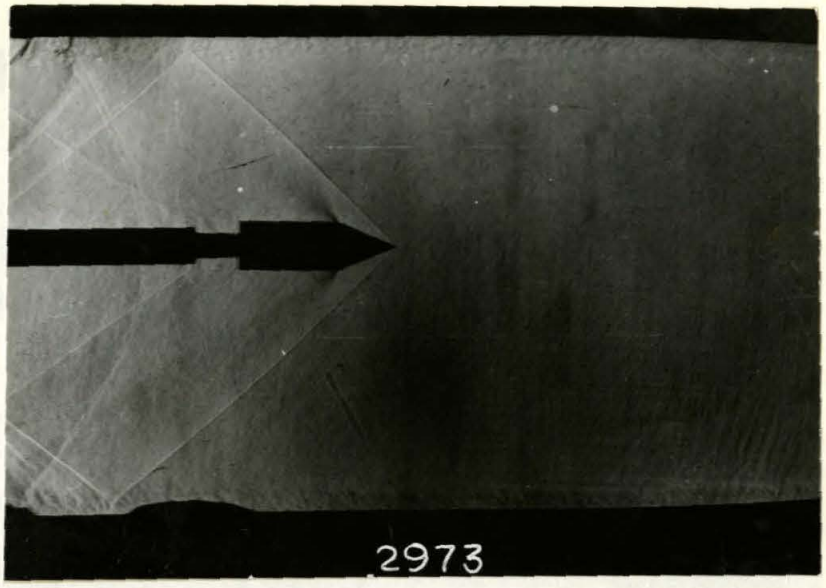

Fig. 35

45° Cone, M = 1.71

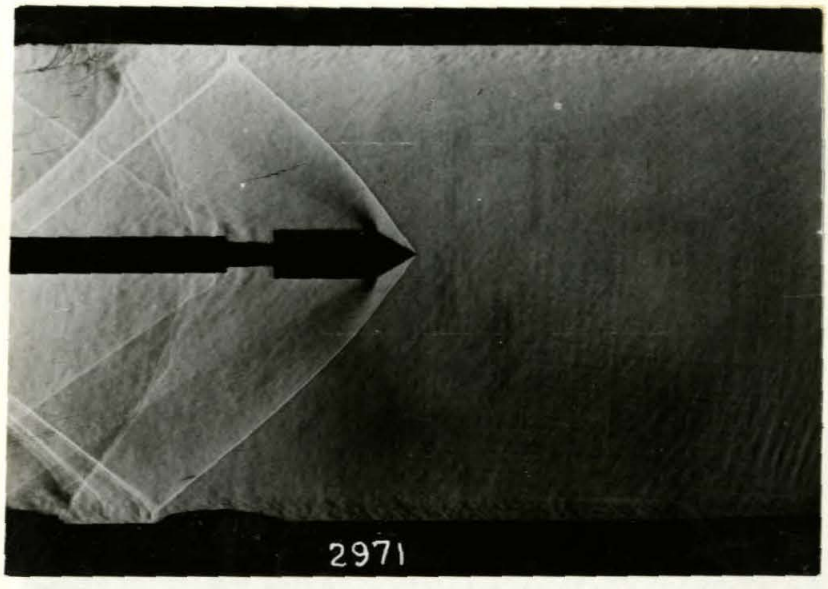

Fig. 36

60° Cone, M = 1.71

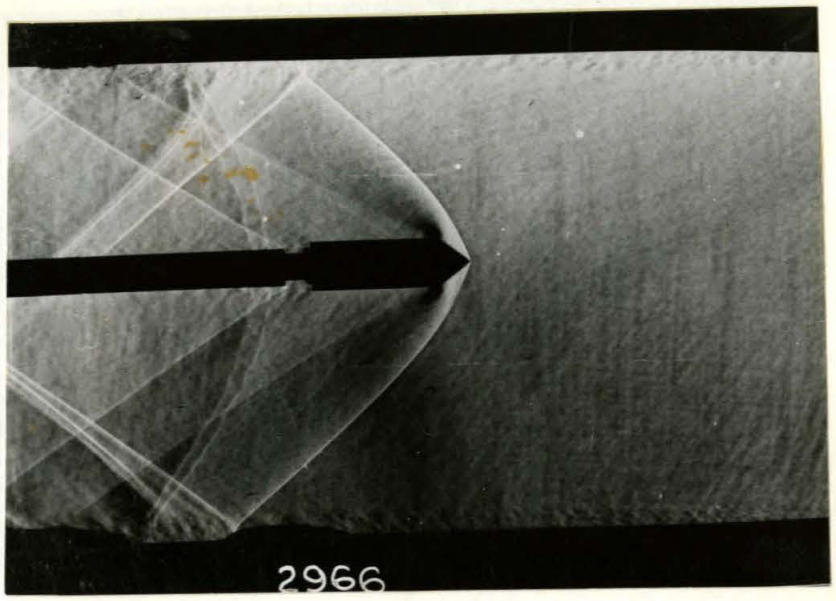

Fig. 37

75° Cone, M = 1.71

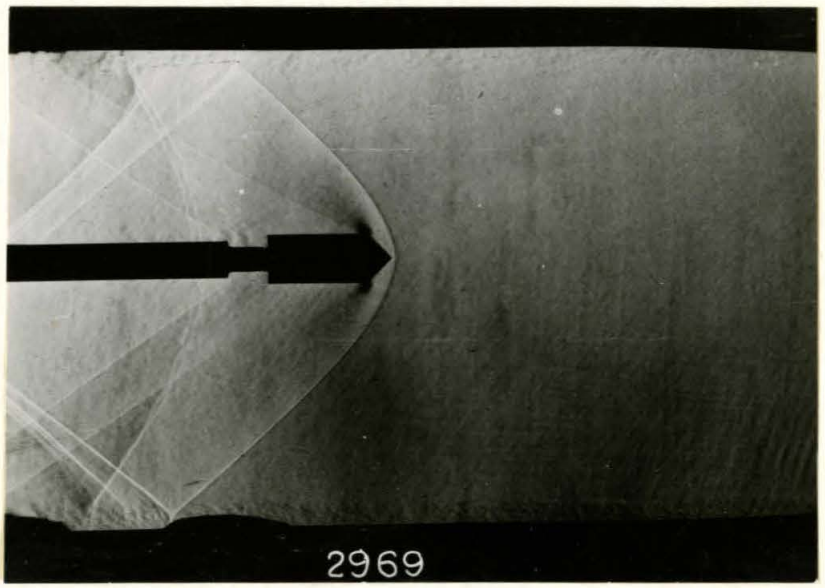

Fig. 38

90° Cone, M = 1.71

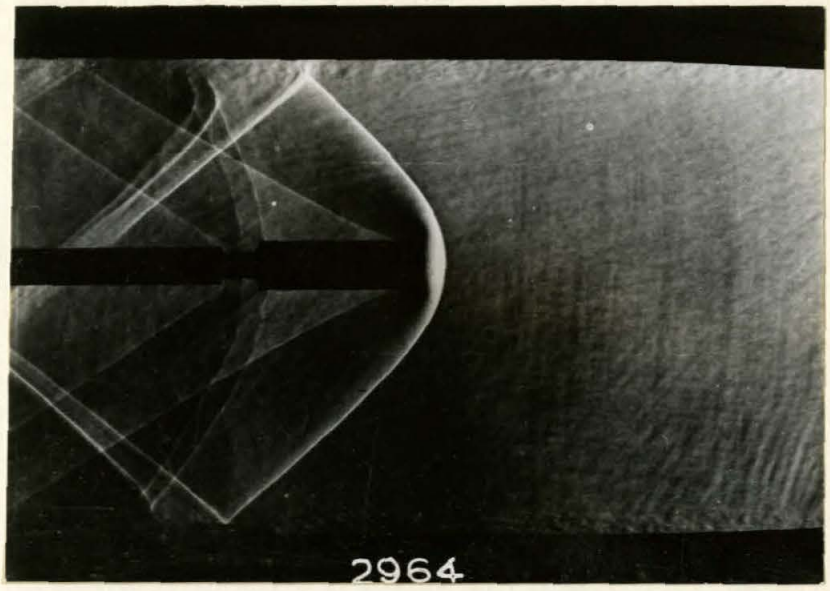

Fig. 39

Blunt Cylinder, M = 1.71

FIG. 40: 75° CONE $M_1 = 1.41$

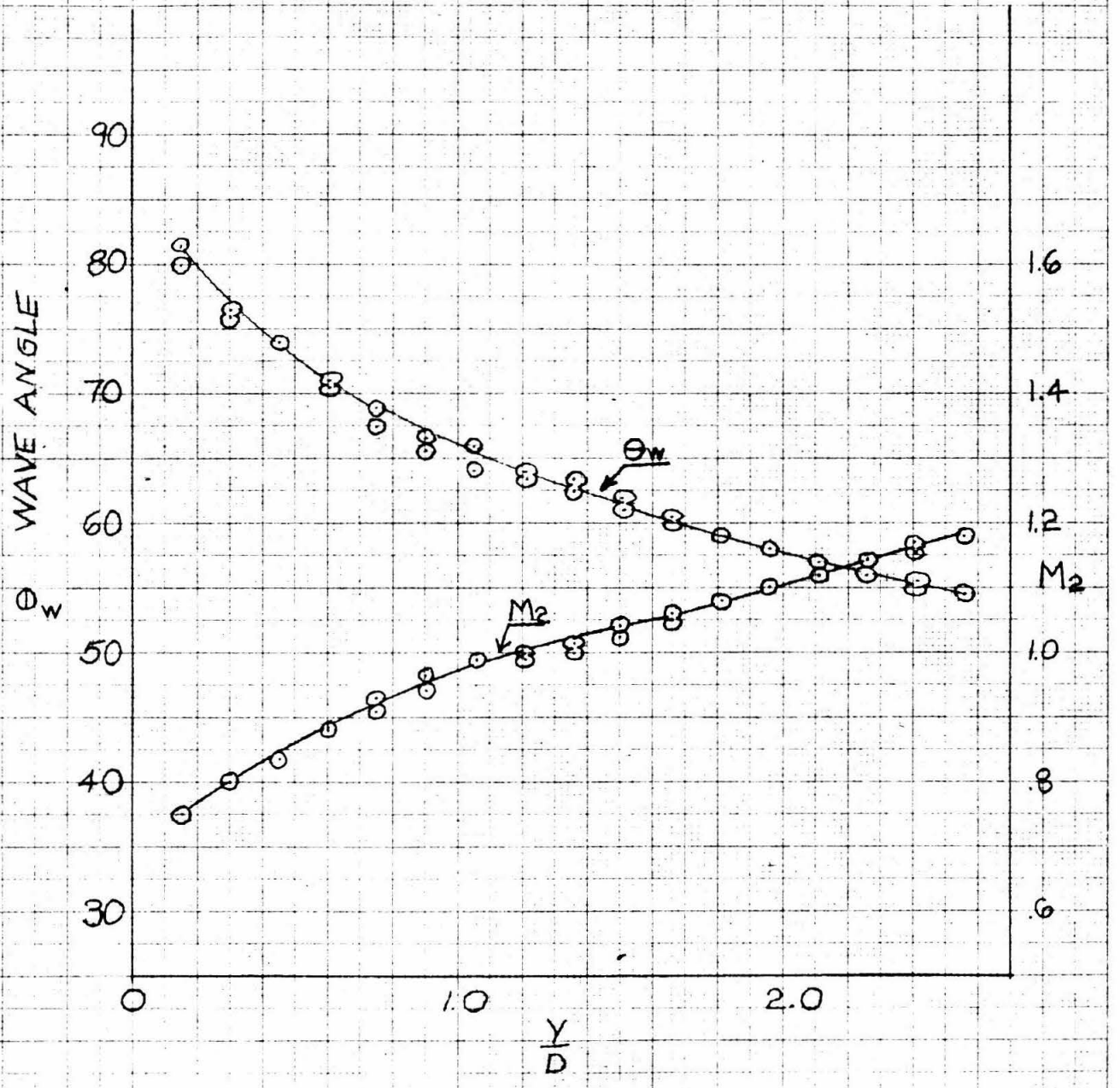

FIG. 41: 75° CONE $M_1 = 1.49$

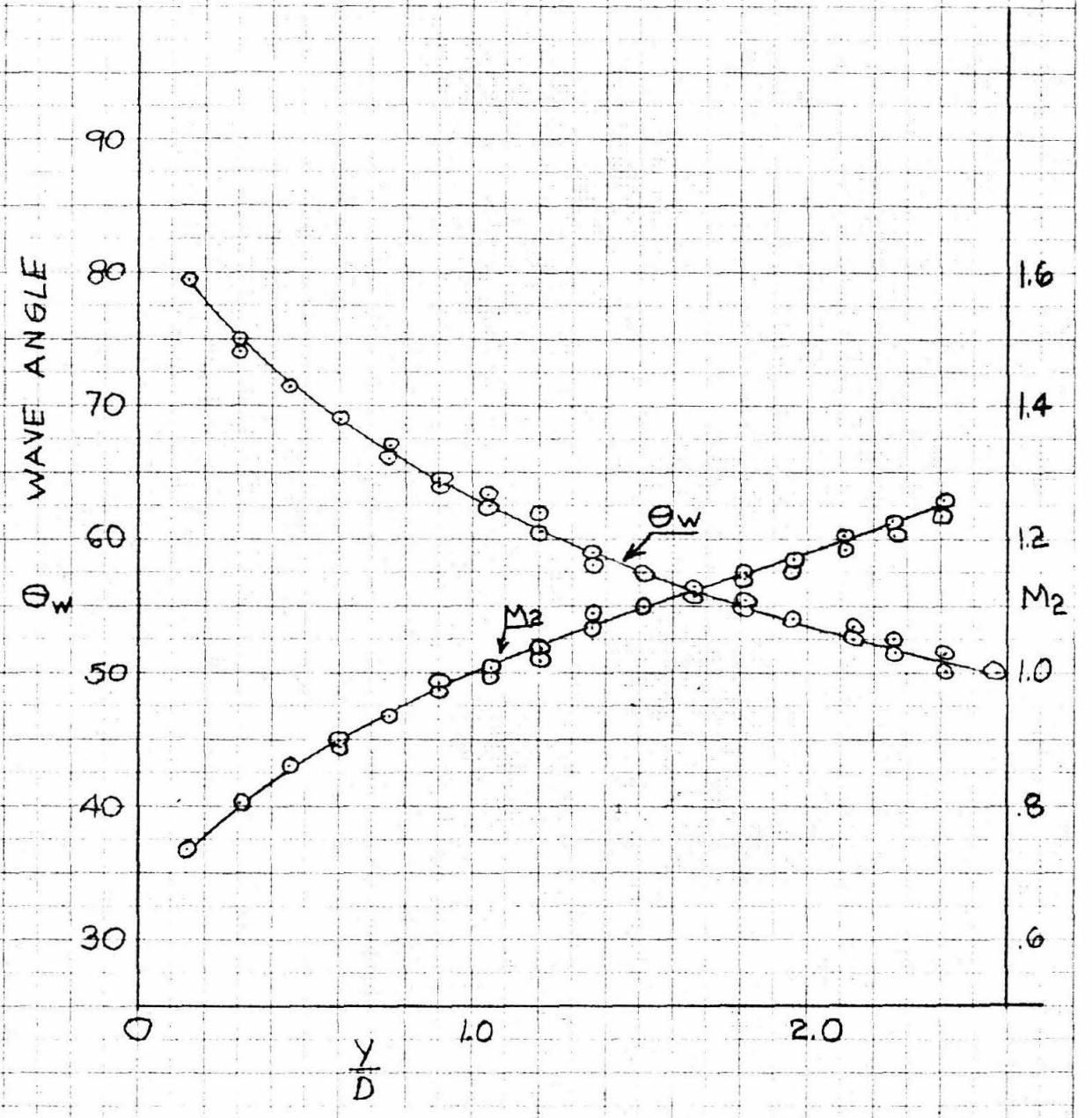

FIG. 42: 75° CONE $M_1 = 1.58$

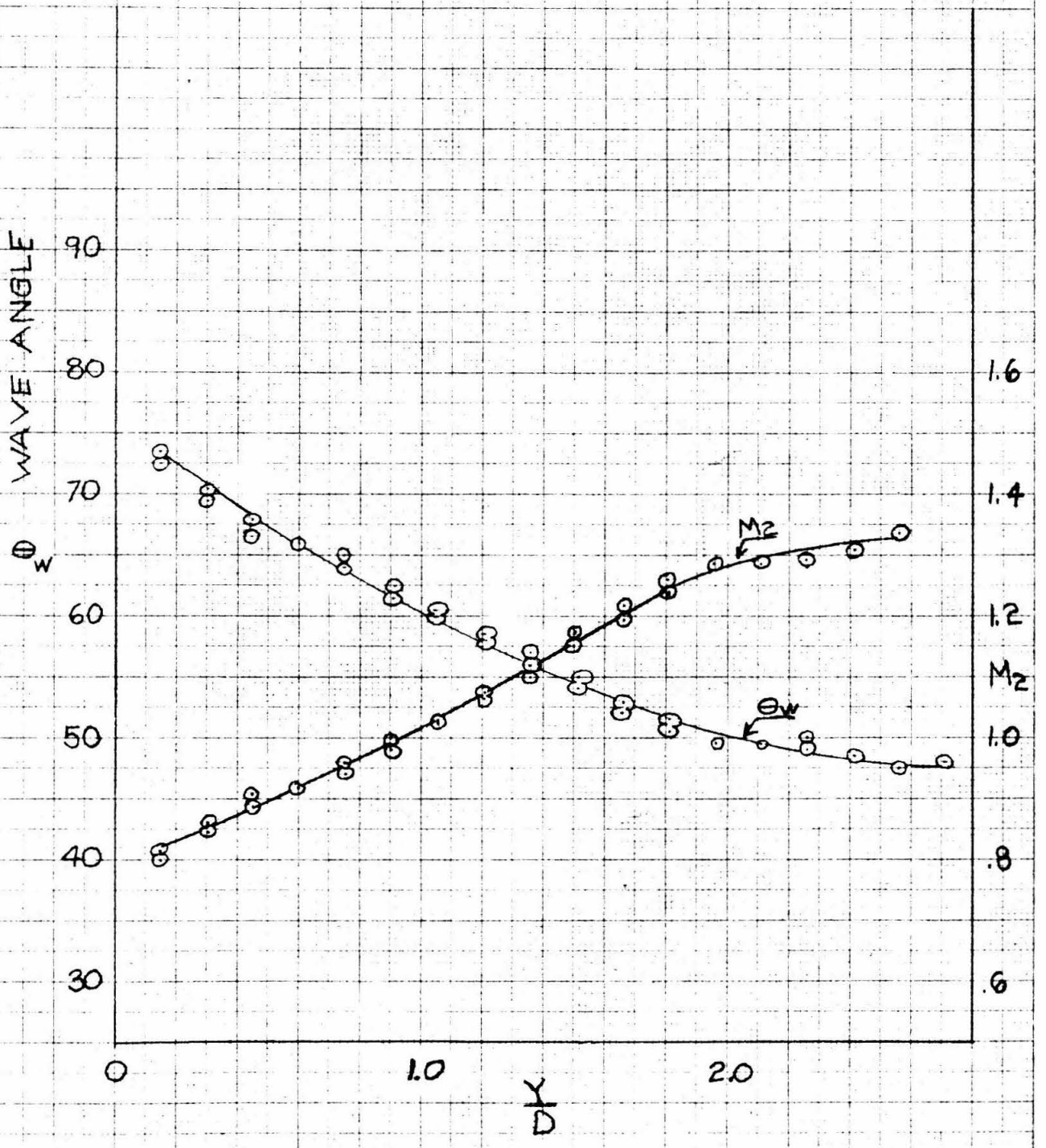

FIG. 43
75° CONE
M = 1.71

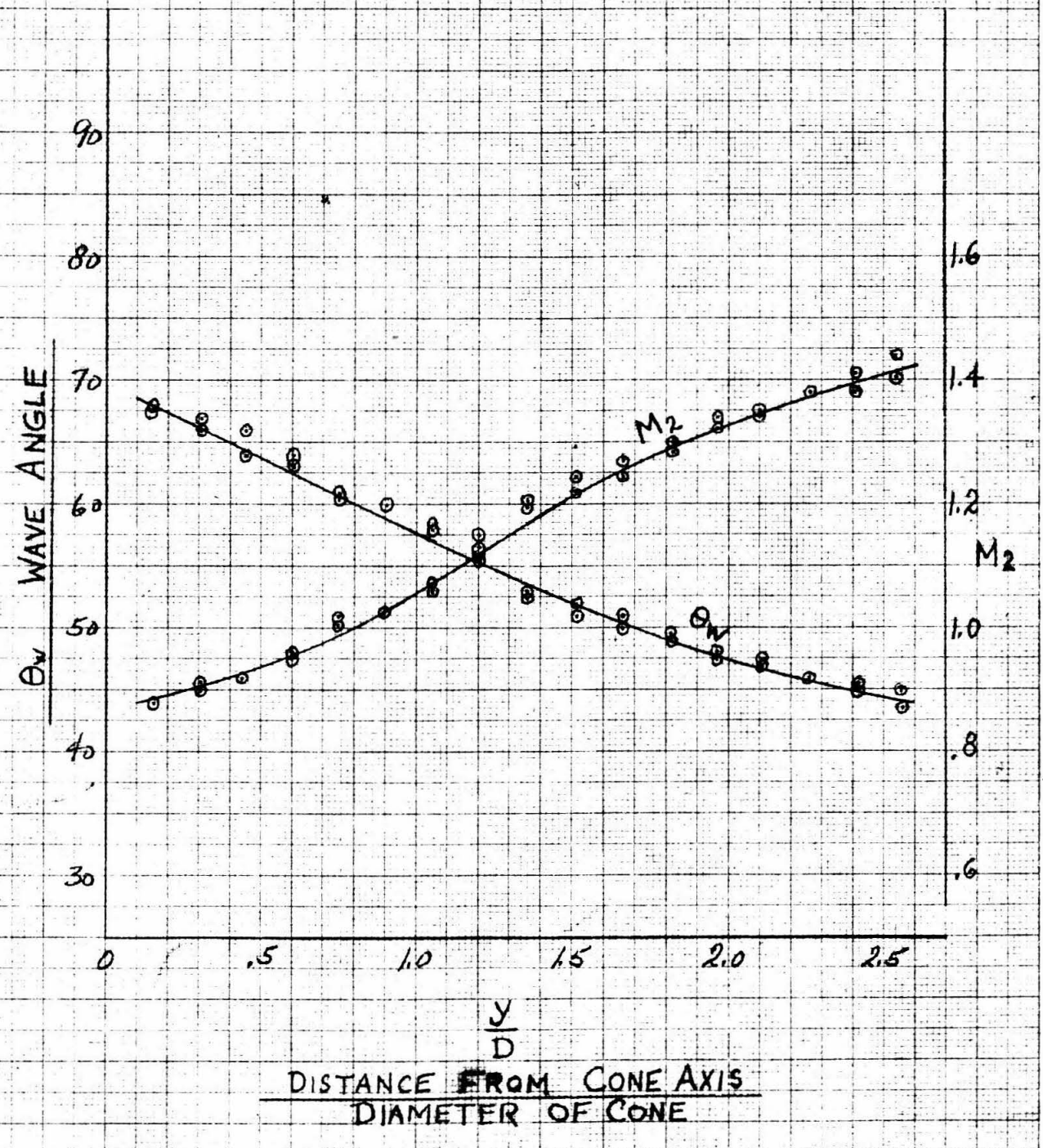

FIG. 44
75° CONE
$M_1 = 1.83$

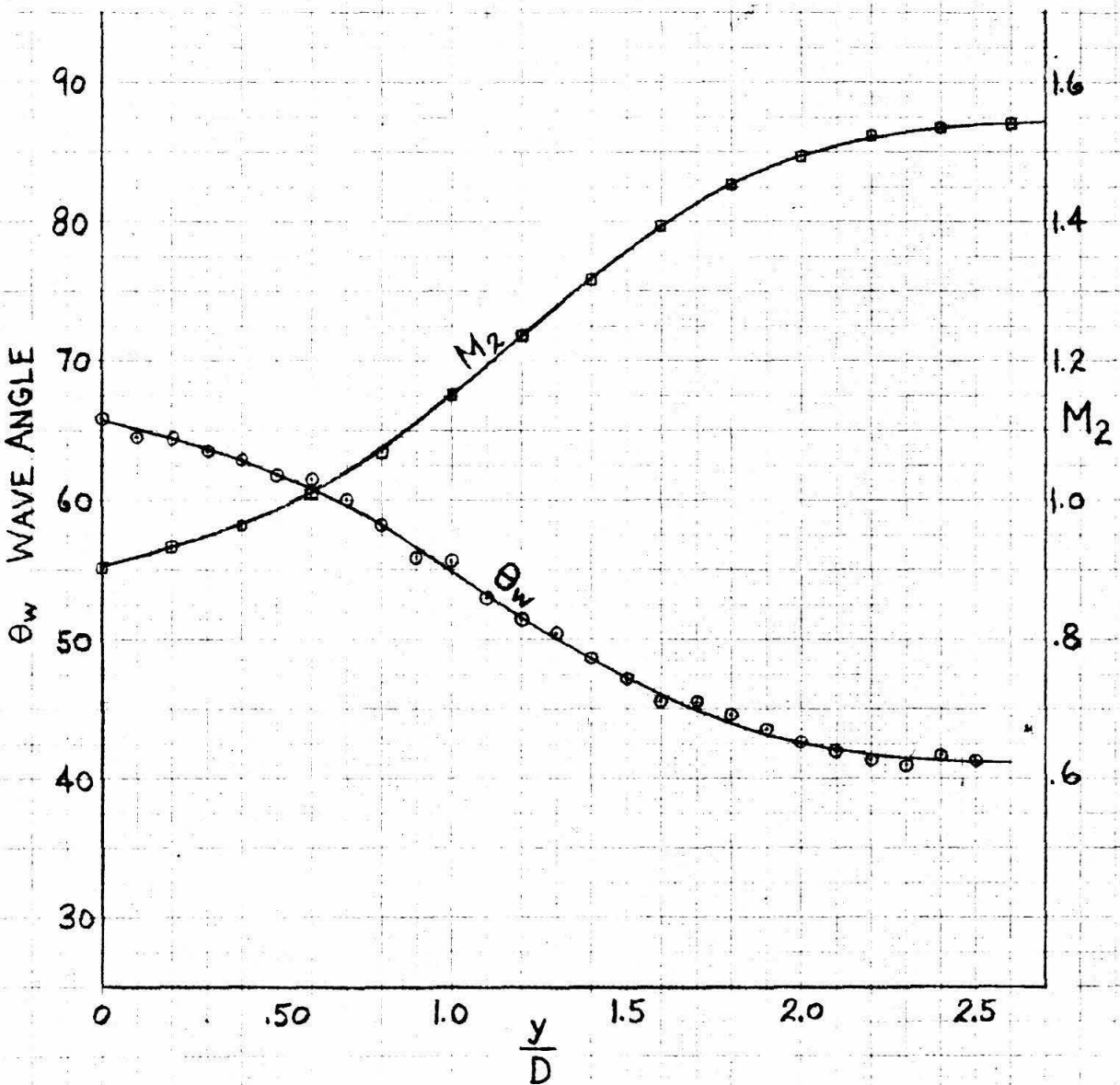

FIG. 45: 75° CONE $M_1 = 1.99$

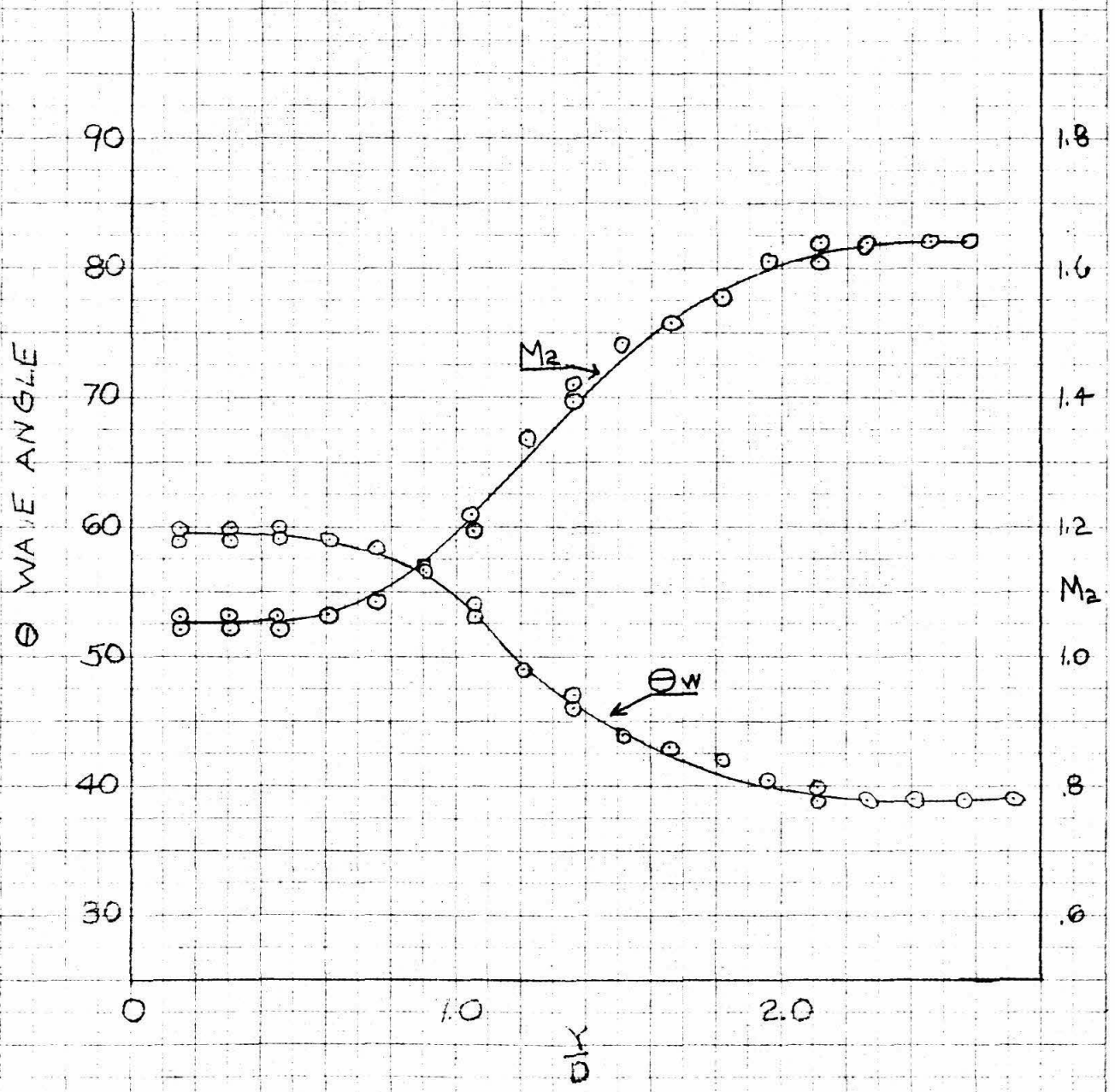

FIG. 46 M_2 SUMMARY FOR 75° CONE

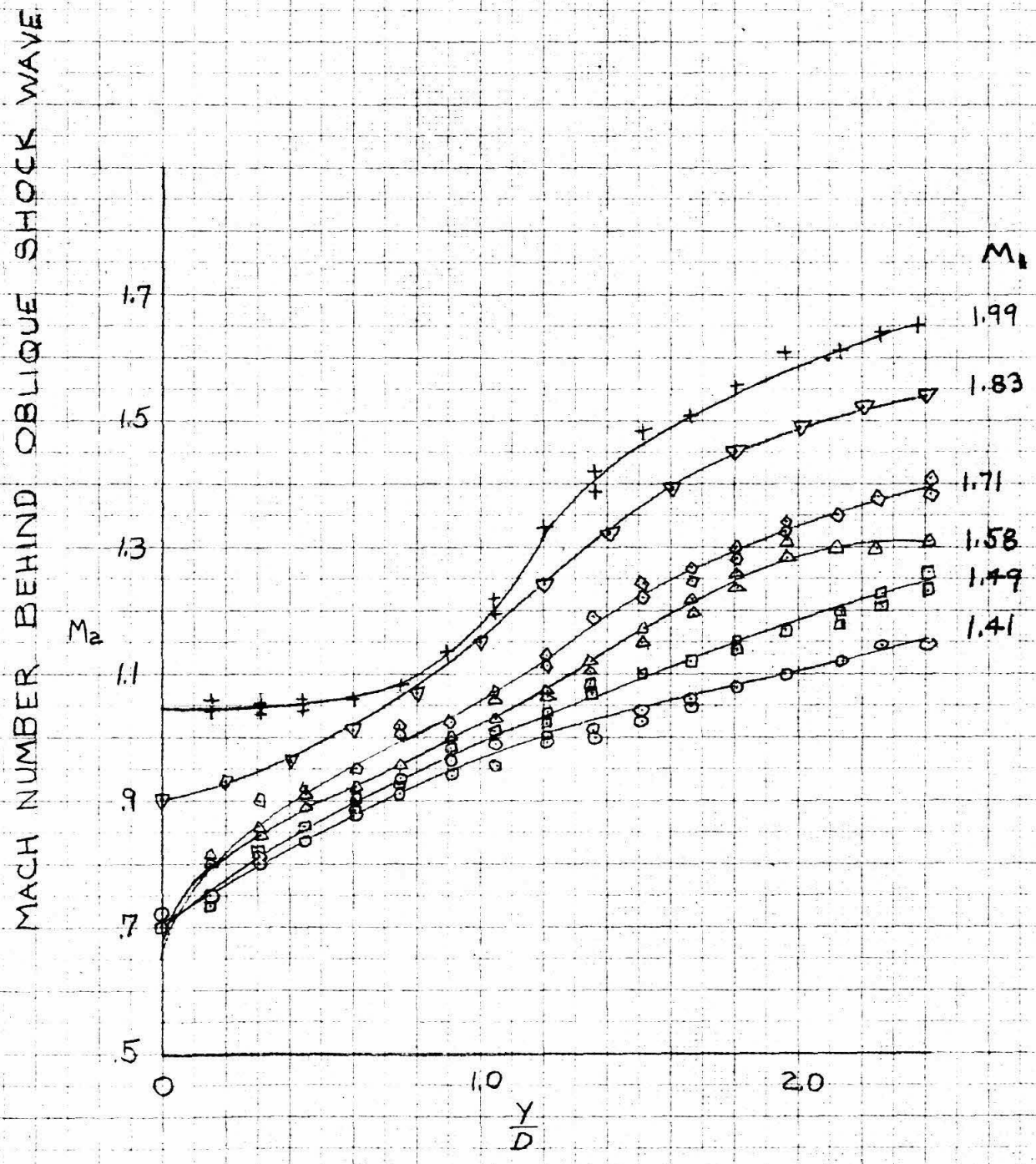

FIG.47 BLUNT CYLINDER $M_1 = 1.41$

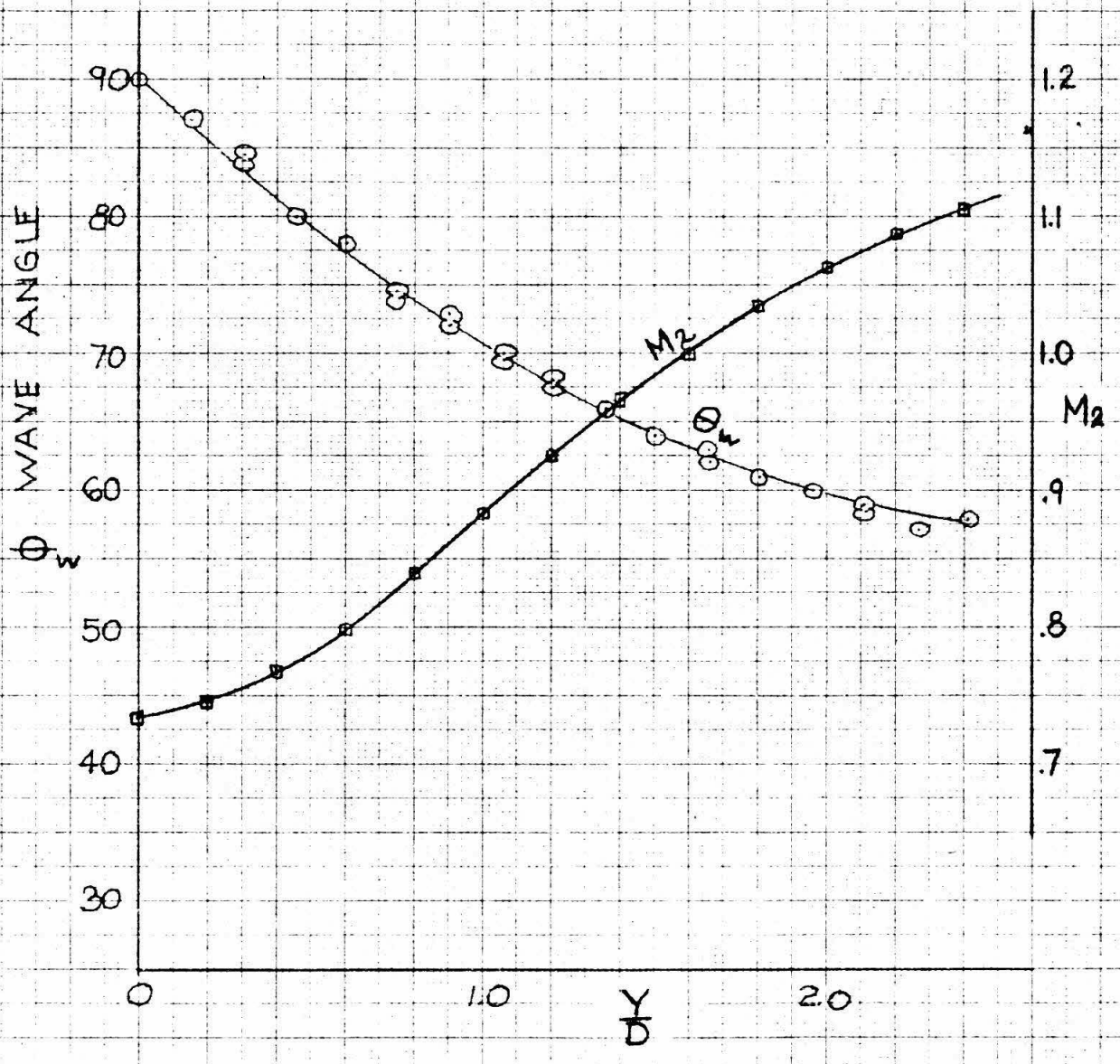

FIG.48 BLUNT CYLINDER $M_1 = 1.49$

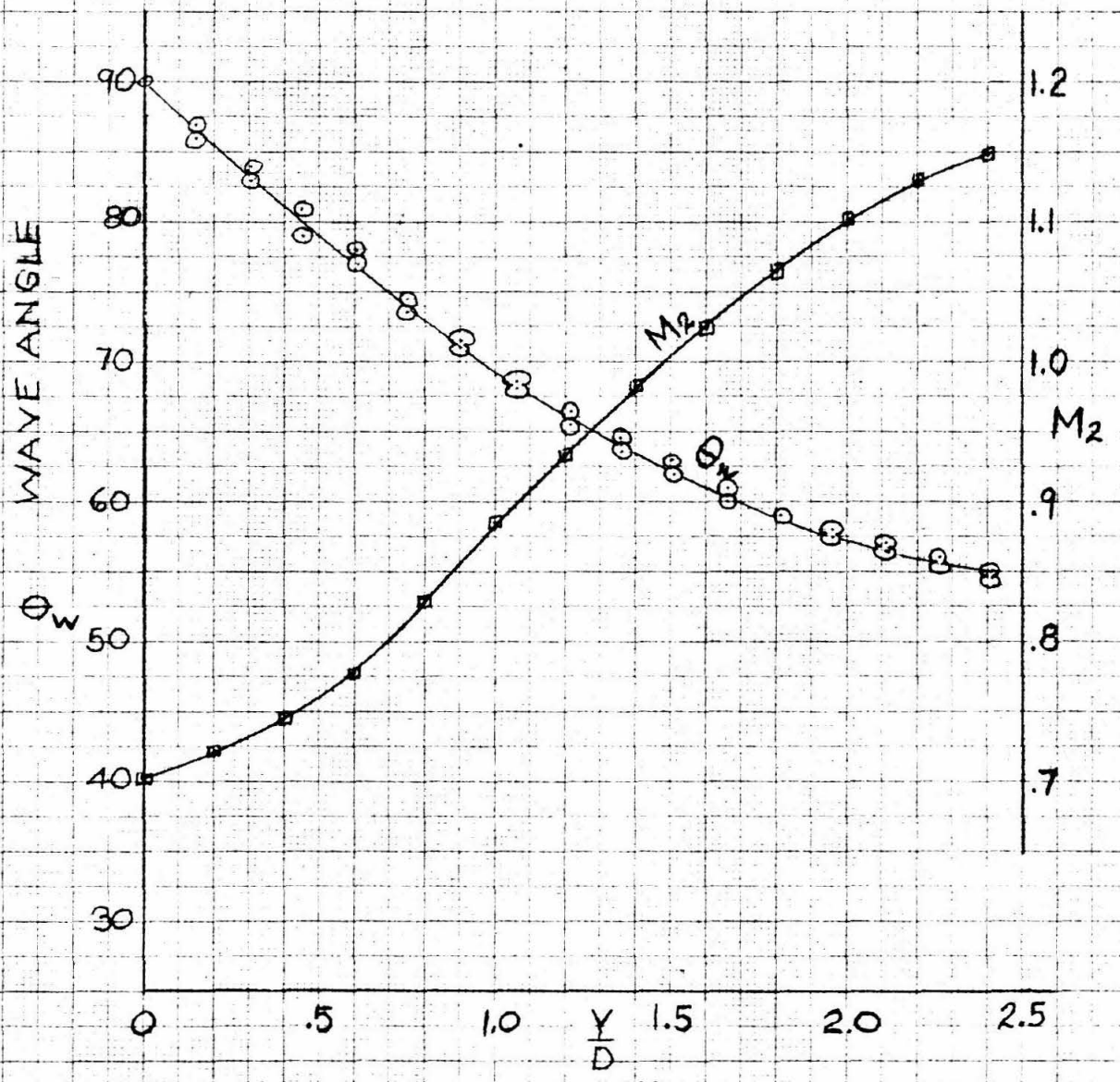

FIG. 49 BLUNT CYLINDER $M_1 = 1.58$

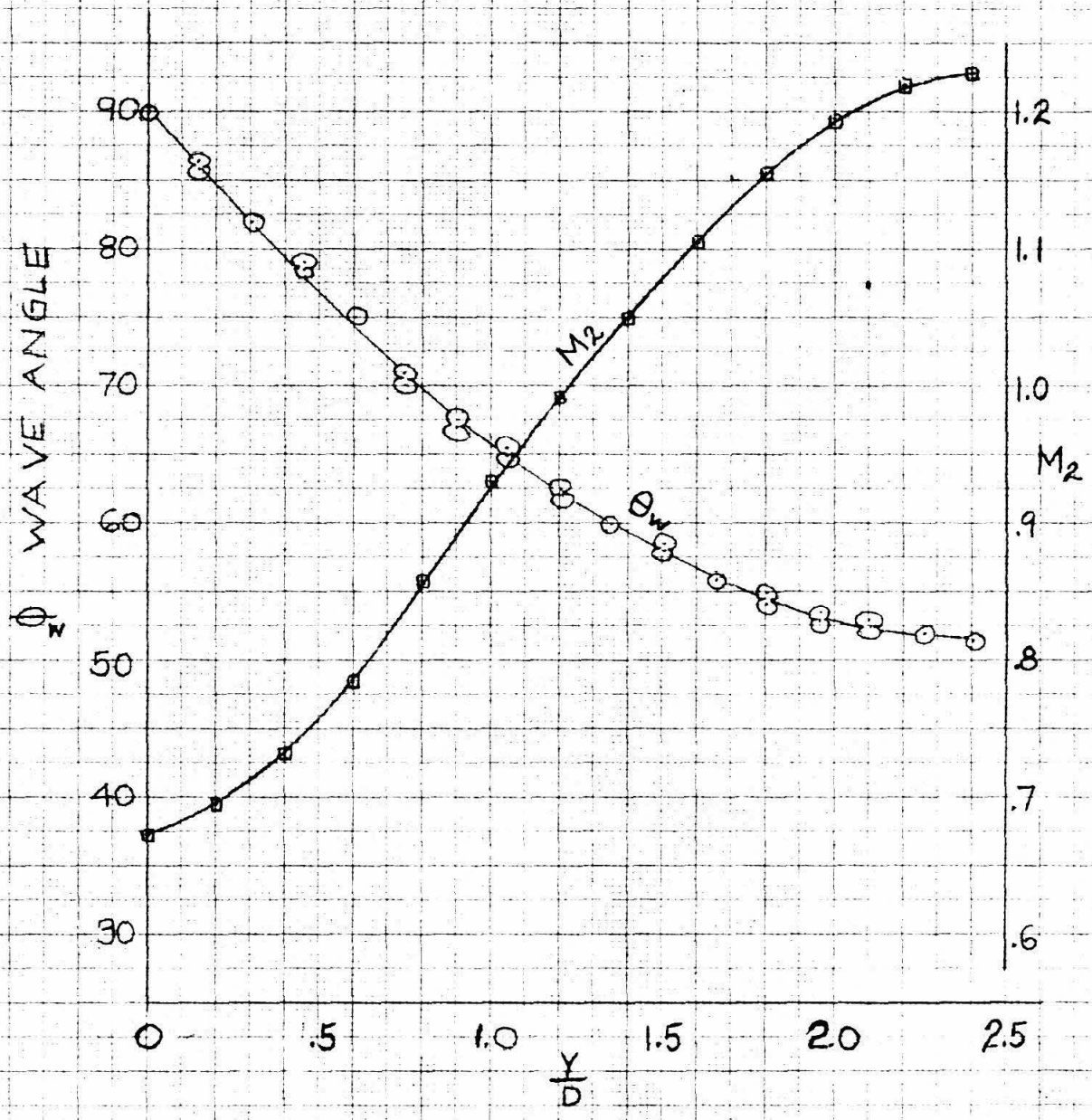

FIG. 50 BLUNT CYLINDER $M_1 = 1.71$

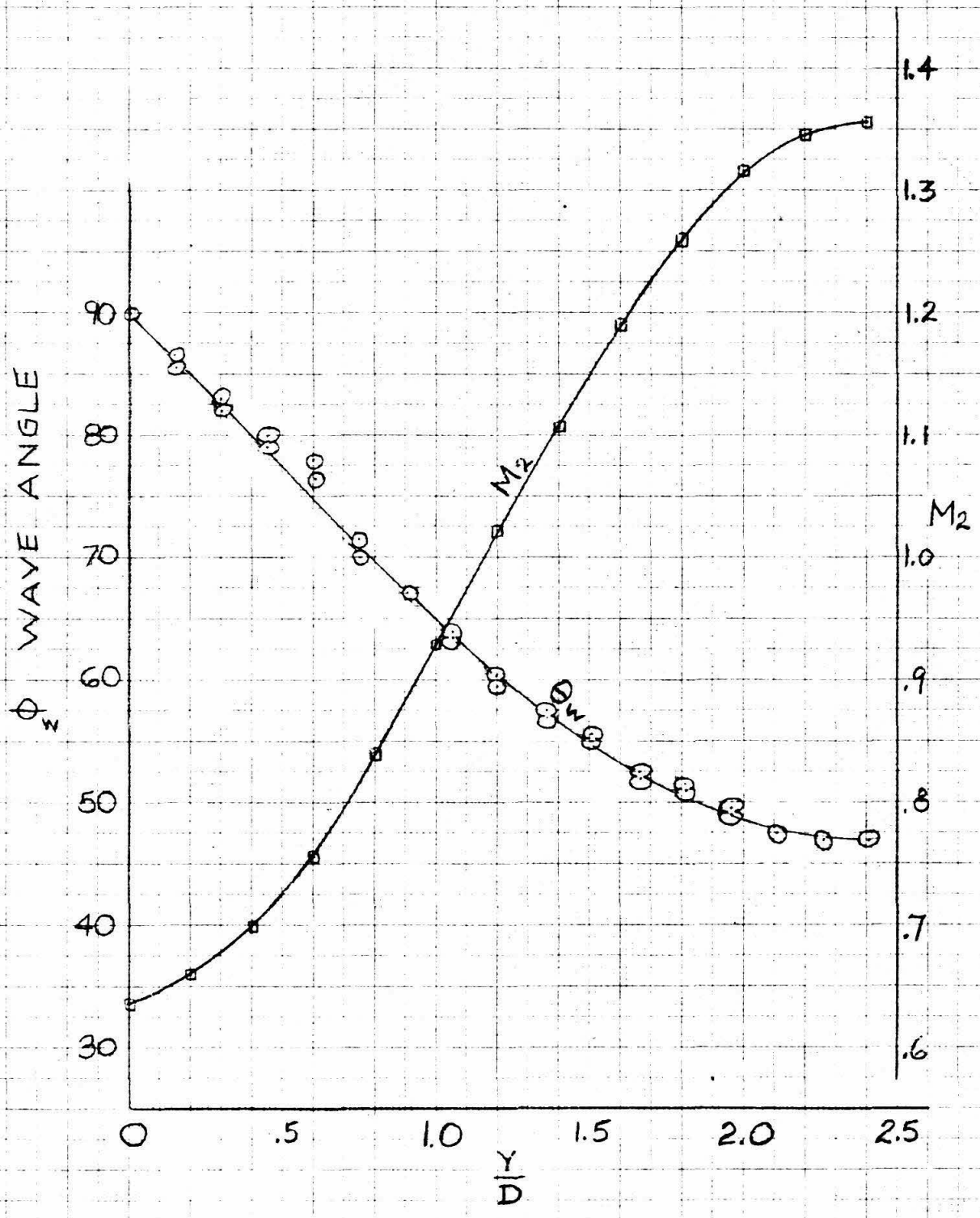

FIG. 51
BLUNT CYLINDER
$M_1 = 1.83$

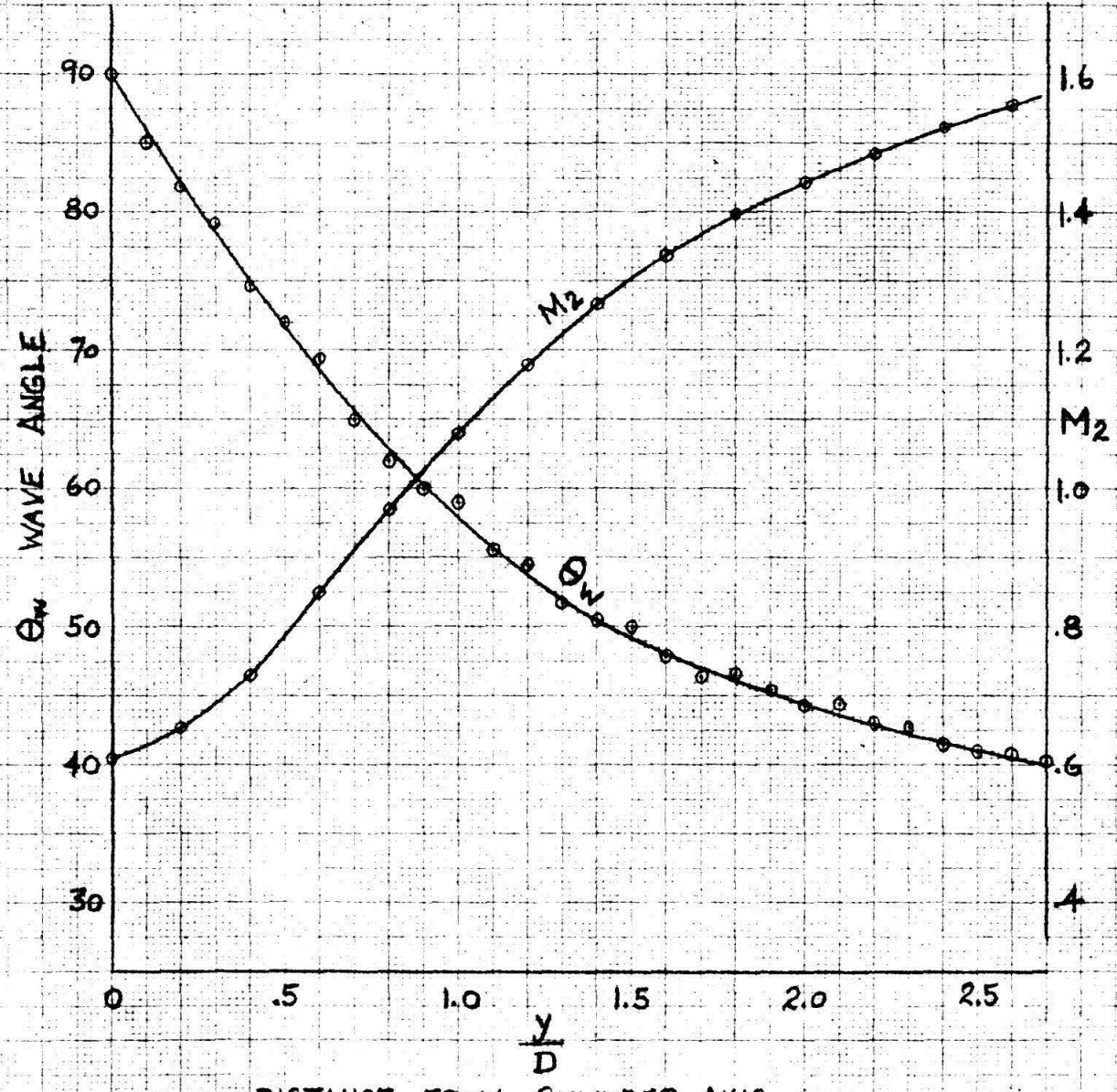

FIG. 52 BLUNT CYLINDER $M_1 = 1.99$

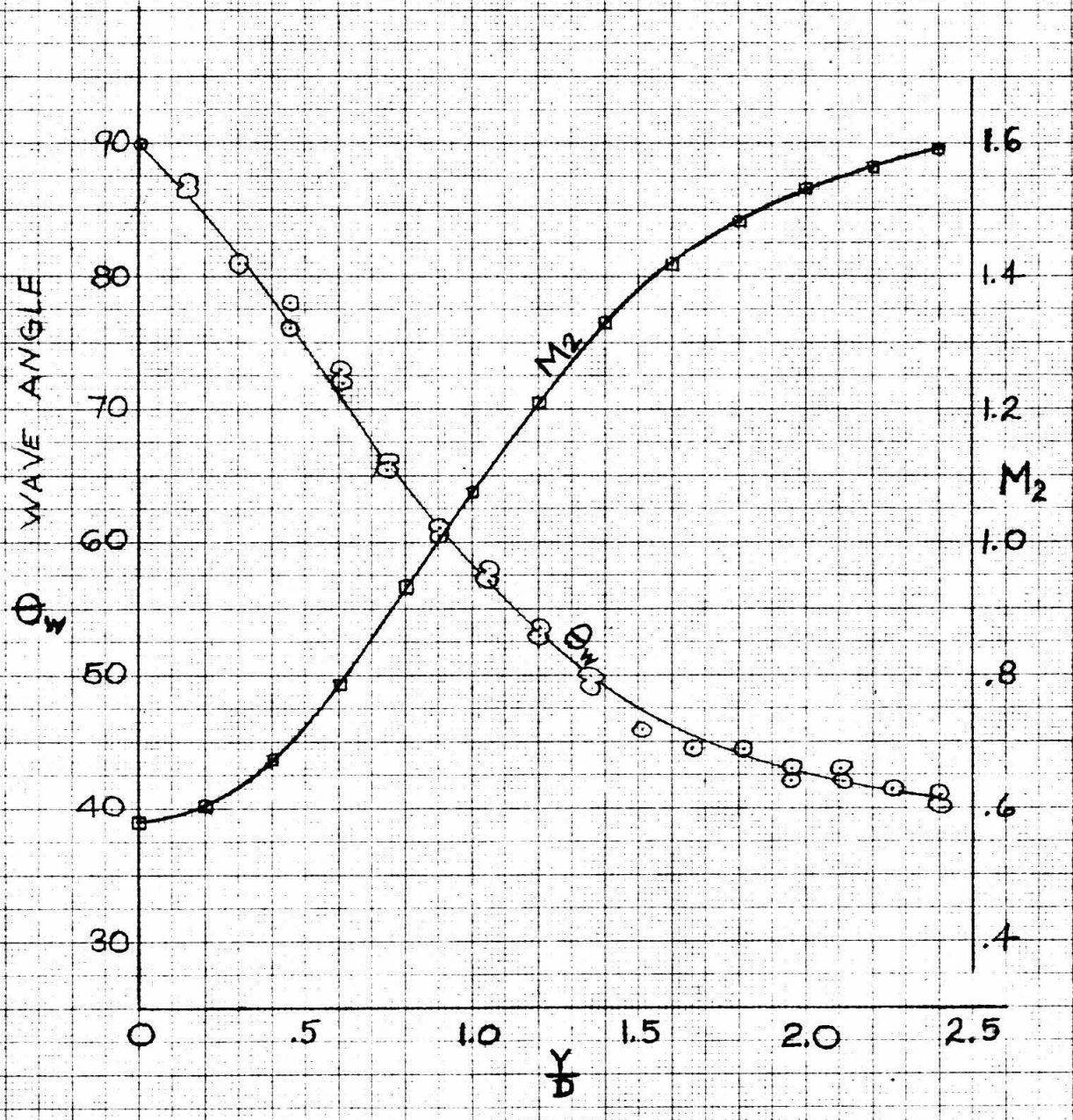

DISTANCE FROM CYLINDER AXIS
DIAMETER OF CYLINDER

FIG. 53 SUMMARY FOR BLUNT CYLINDER

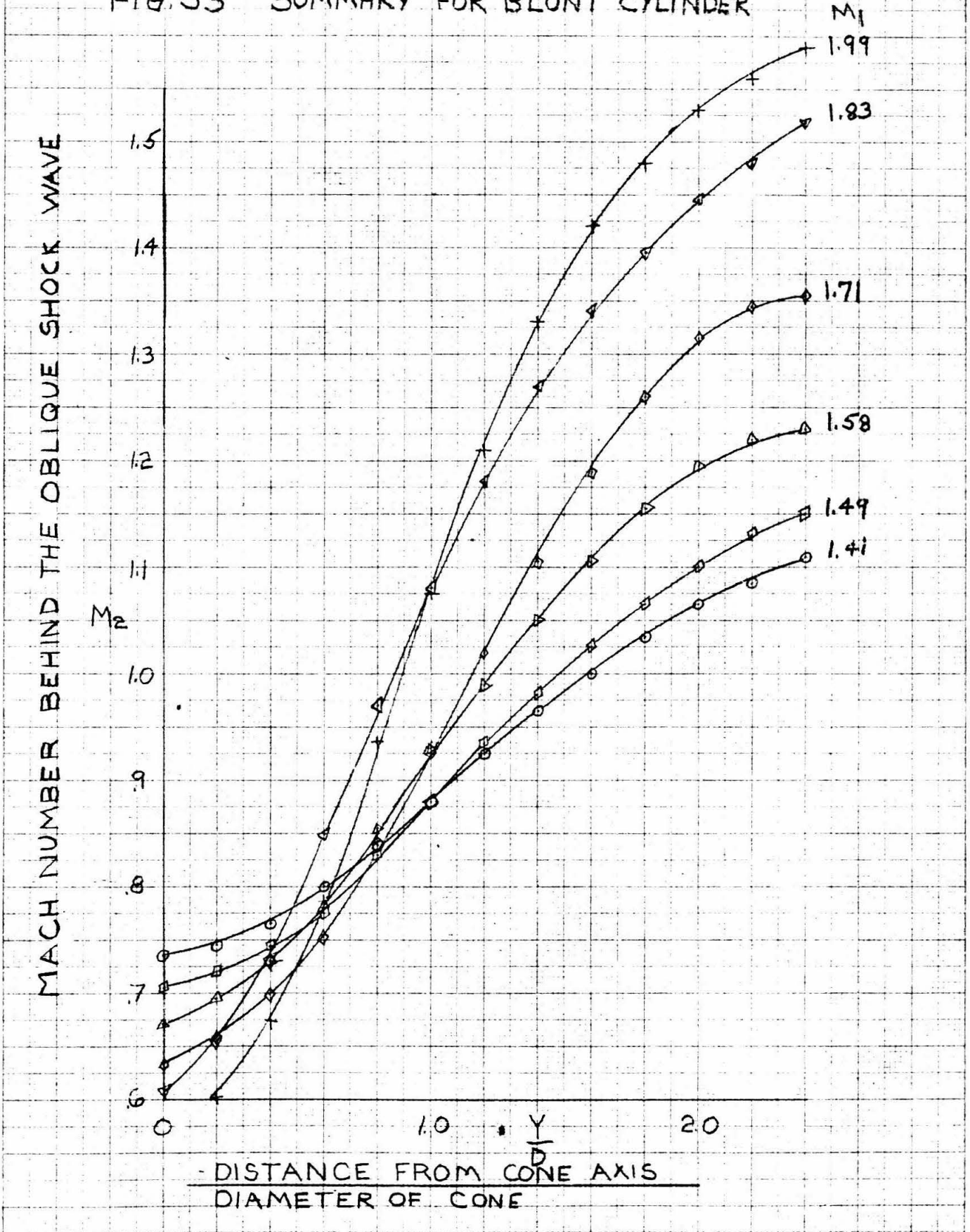

FIG. 54: SHOCK WAVE PATTERN 75° CONE

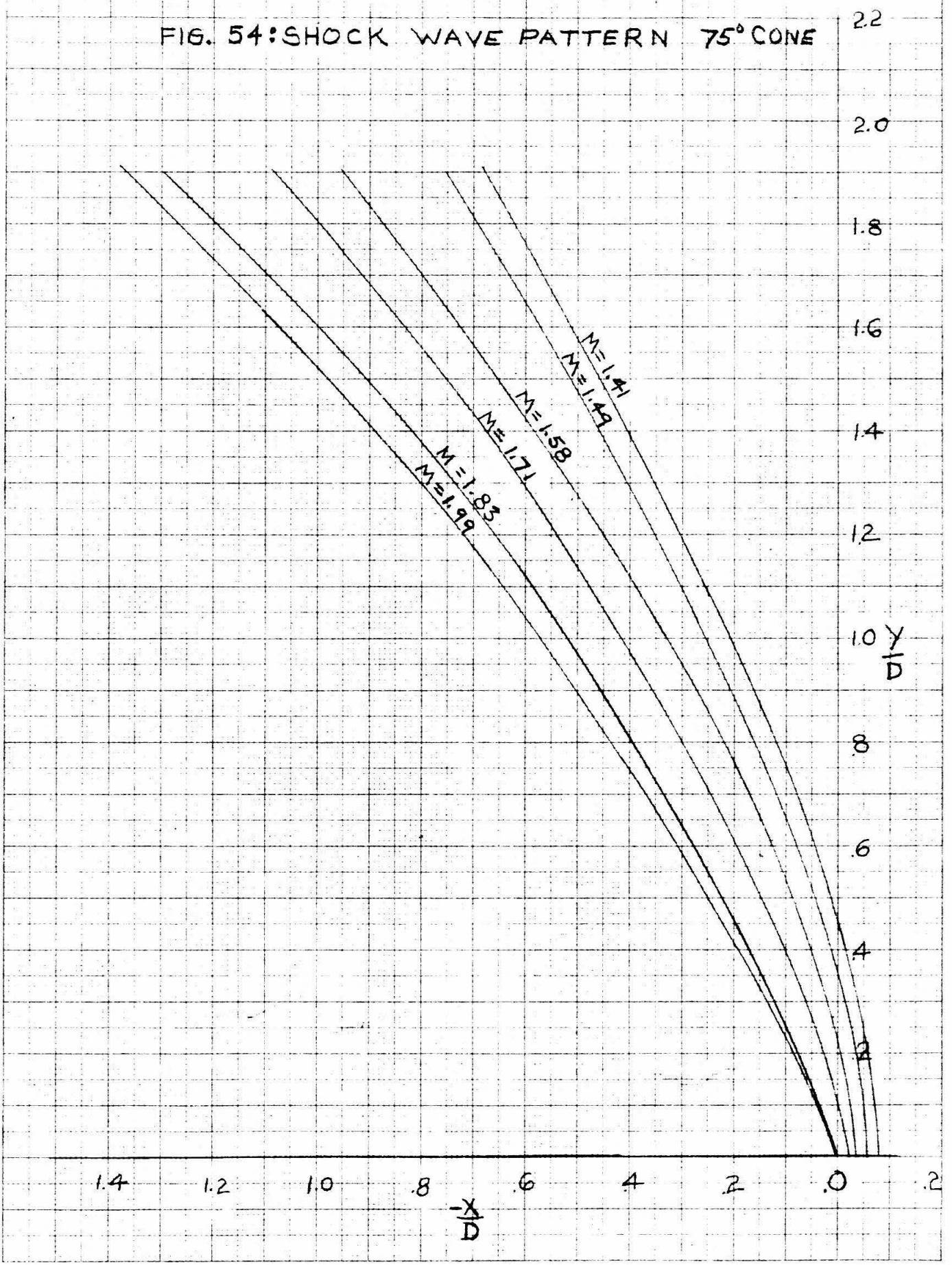

FIG. 55: SHOCK WAVE PATTERN BLUNT CONE

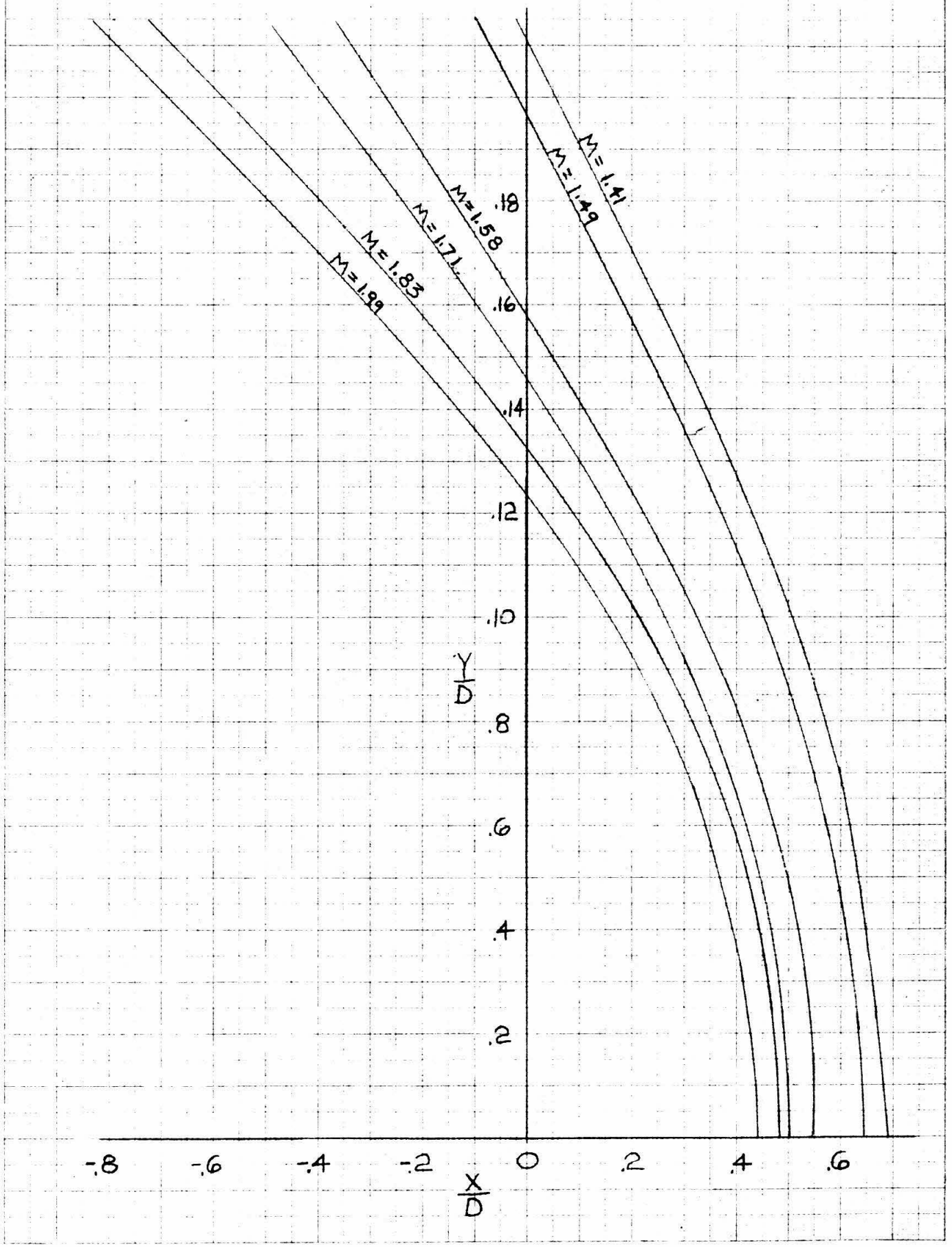

FIG. 56: SHOCK WAVE PATTERN
$M_1 = 1.71$

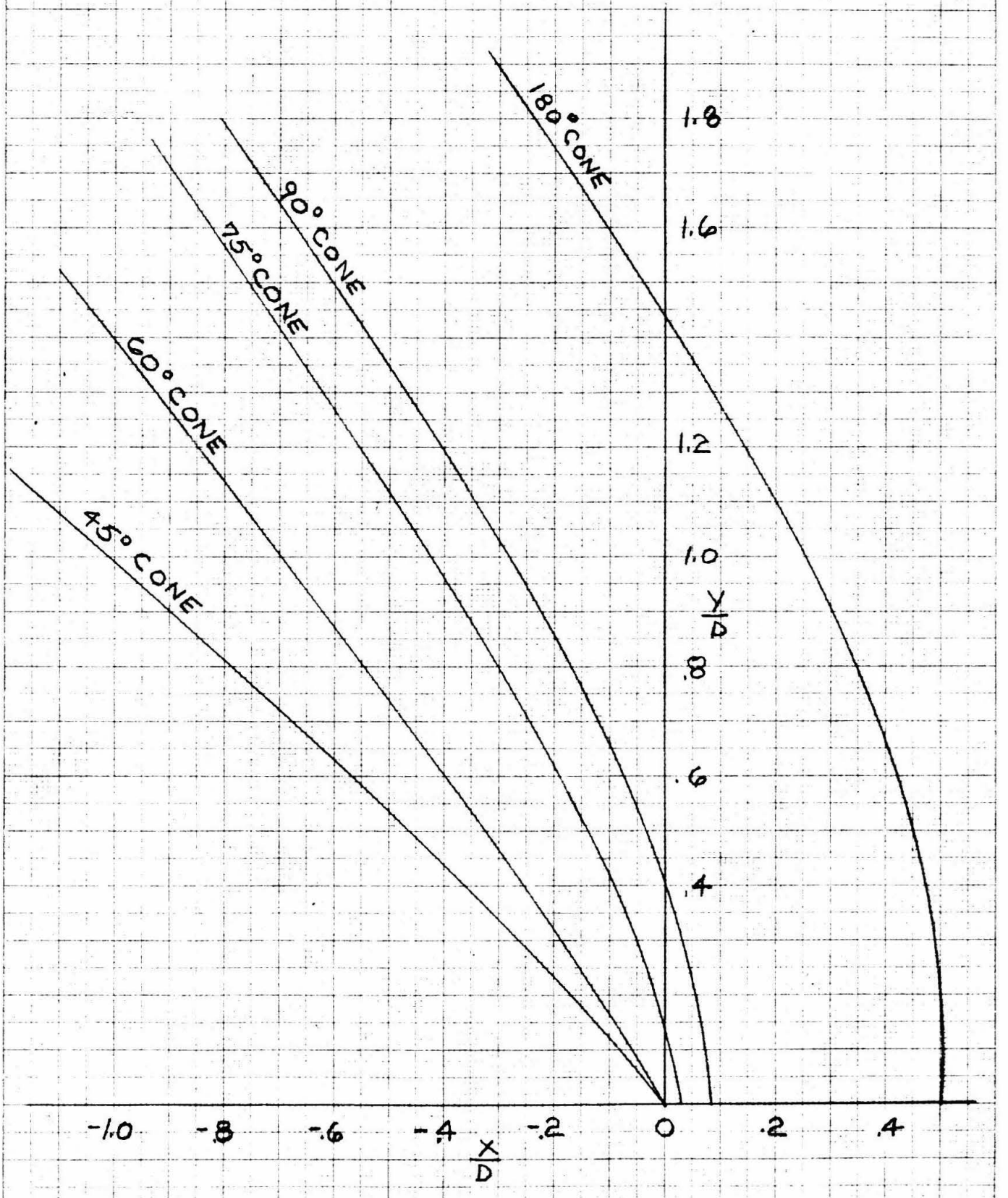

FIG. 57
SHOCK WAVE PATTERN
M = 1.83

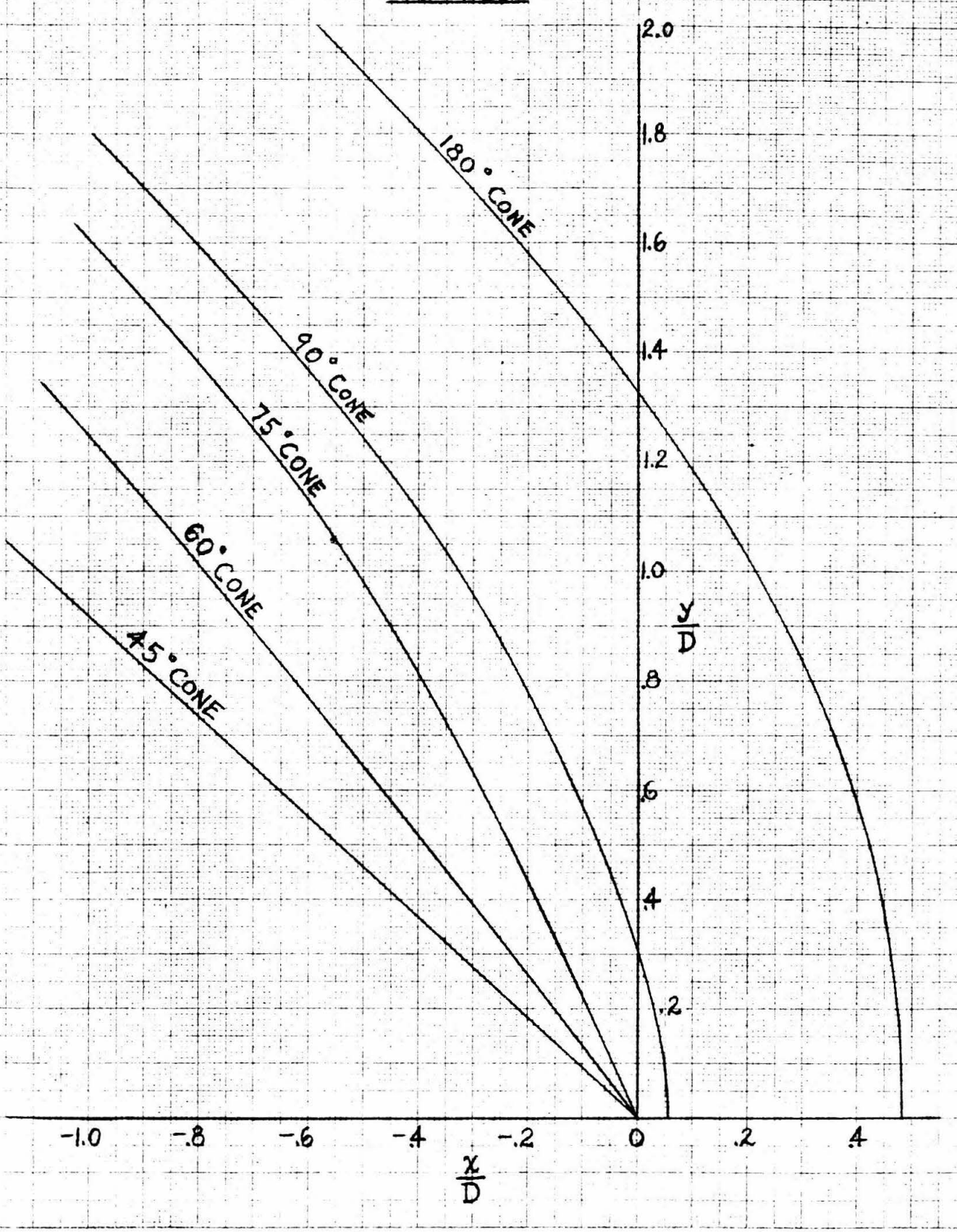

FIG. 58: SHOCK WAVE PATTERN
$M_1 = 1.99$

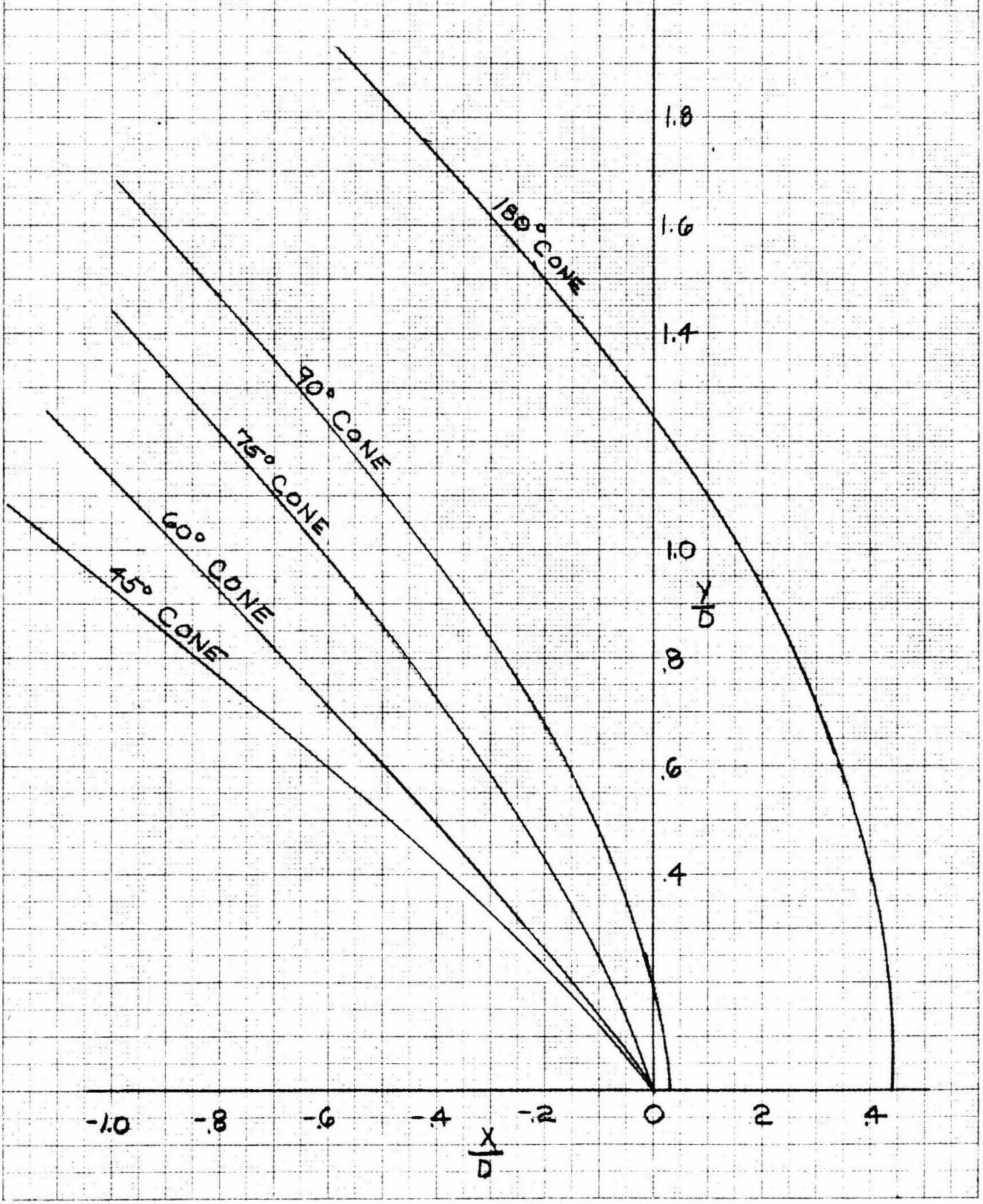

FIG. 59: DETACHED SHOCK WAVE DISTANCE
75° CONE

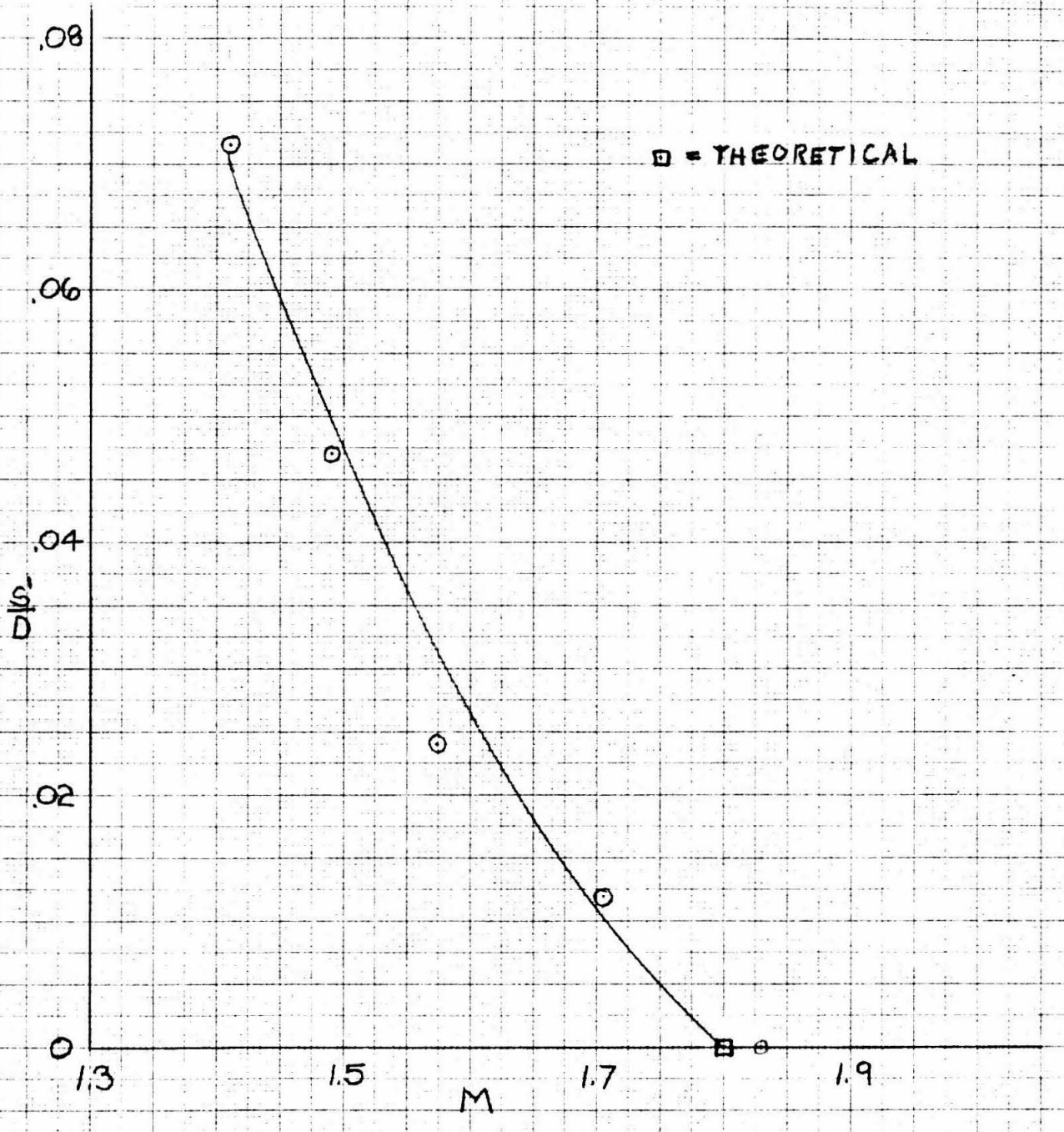

FIG. 60: DETACHED SHOCK WAVE DISTANCE
BLUNT CYLINDER

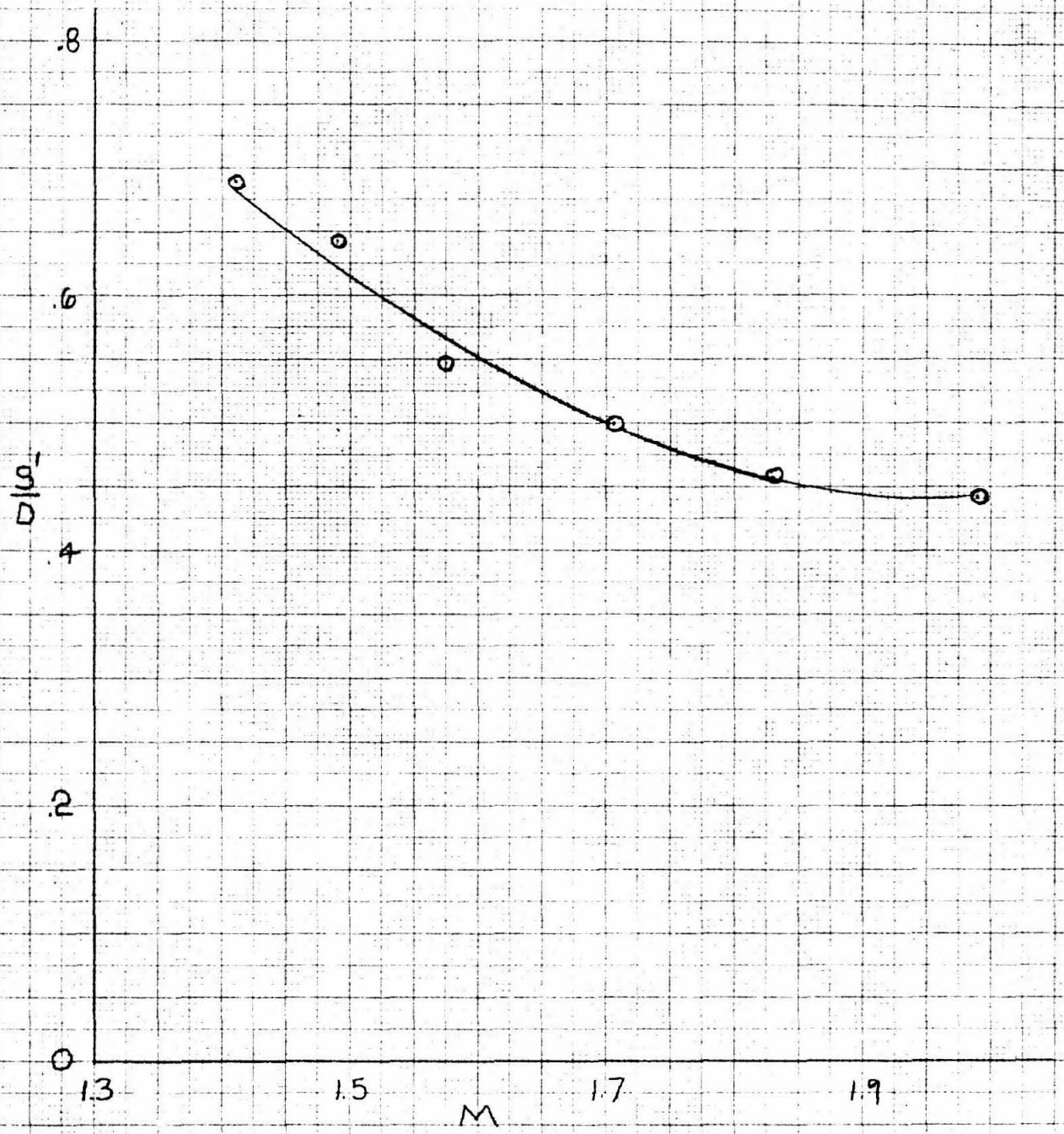

FIG. 61 LOCATION OF $M_2 = 1.00$

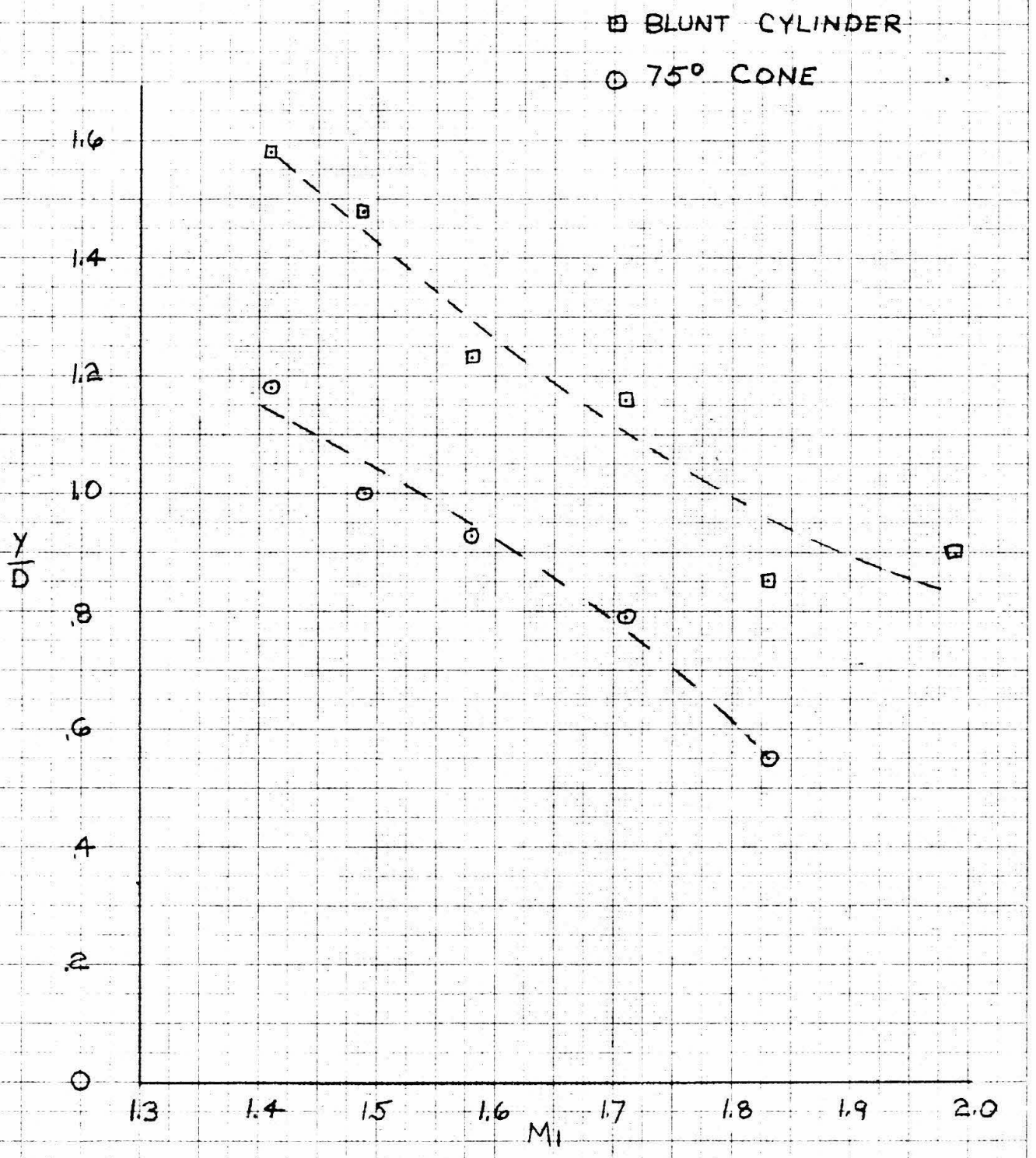

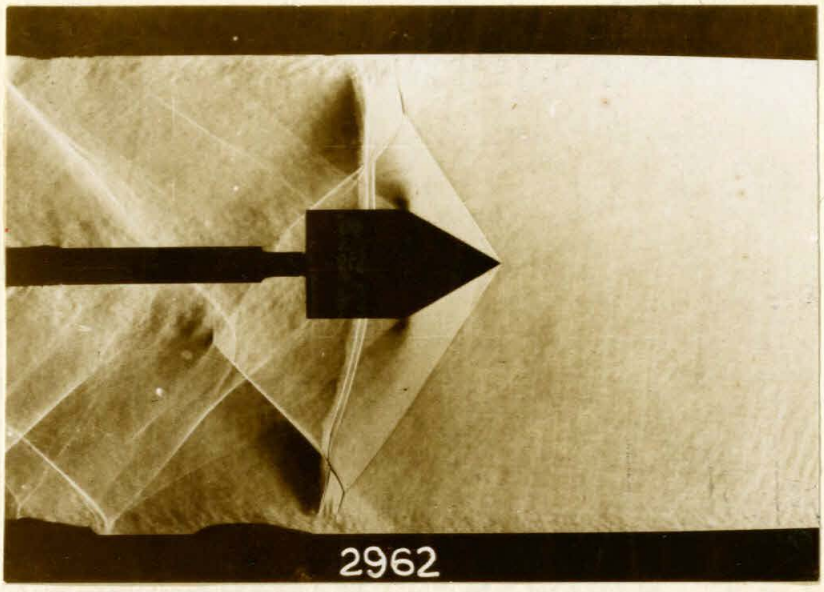

Fig. 62

M = 1.58, D = 9/16" Unblocked

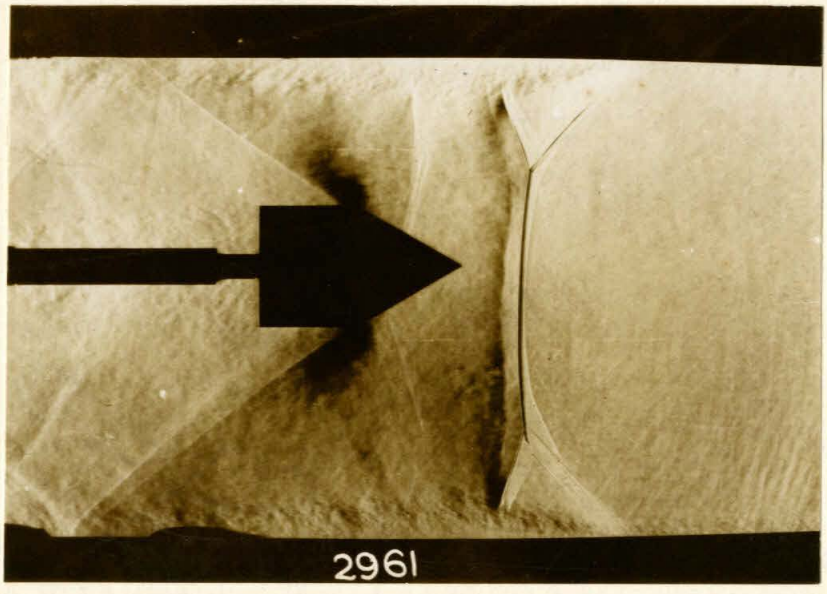

Fig. 63

M = 1.58, D = 10/16" Blocked

FIG. 64

TEST SECTION BLOCKING AREA
2 ½" SUPERSONIC TUNNEL

ΔA = MODEL AREA
A = TEST SECTION AREA
⊙ = EXPERIMENTAL RESULTS

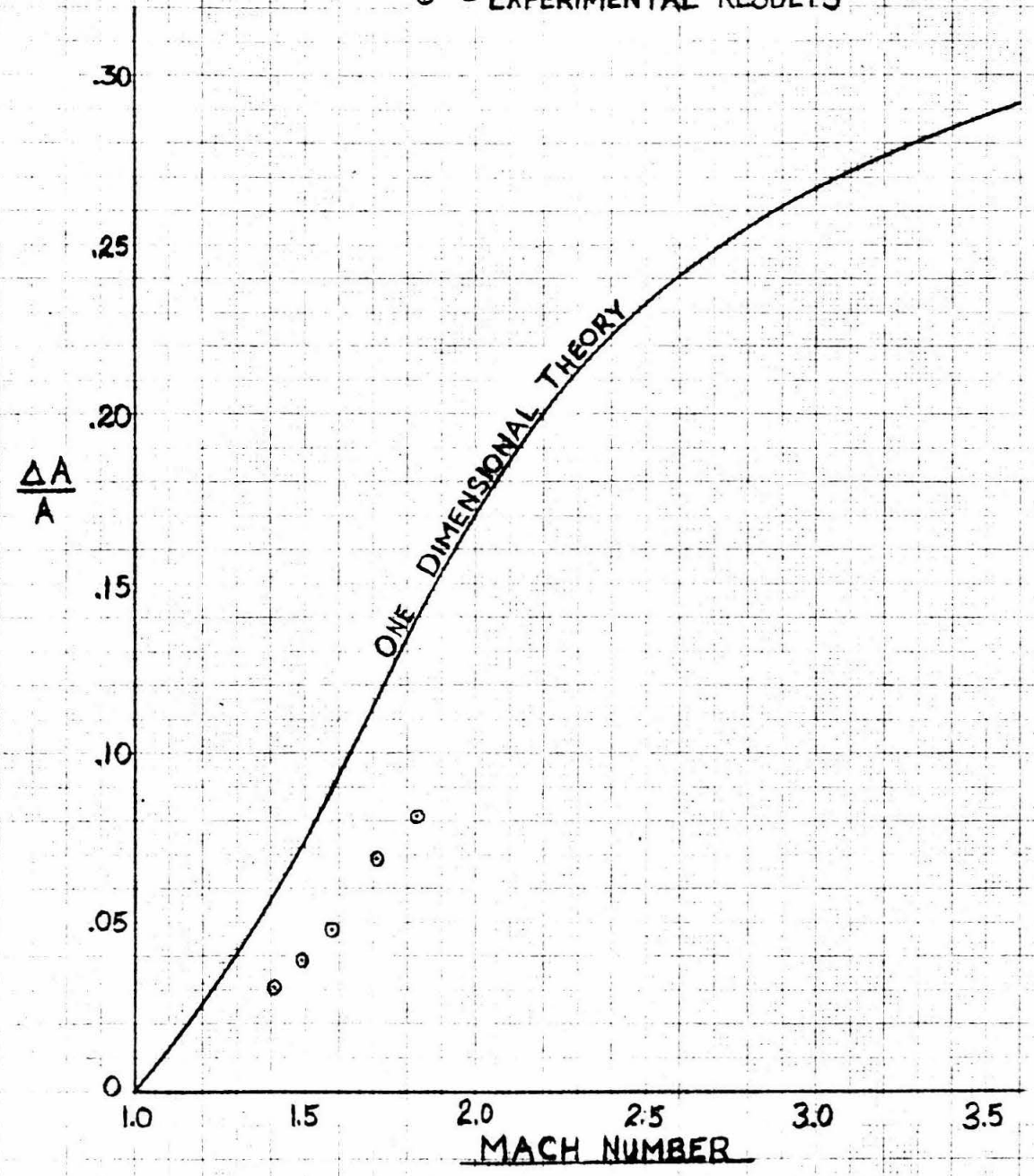

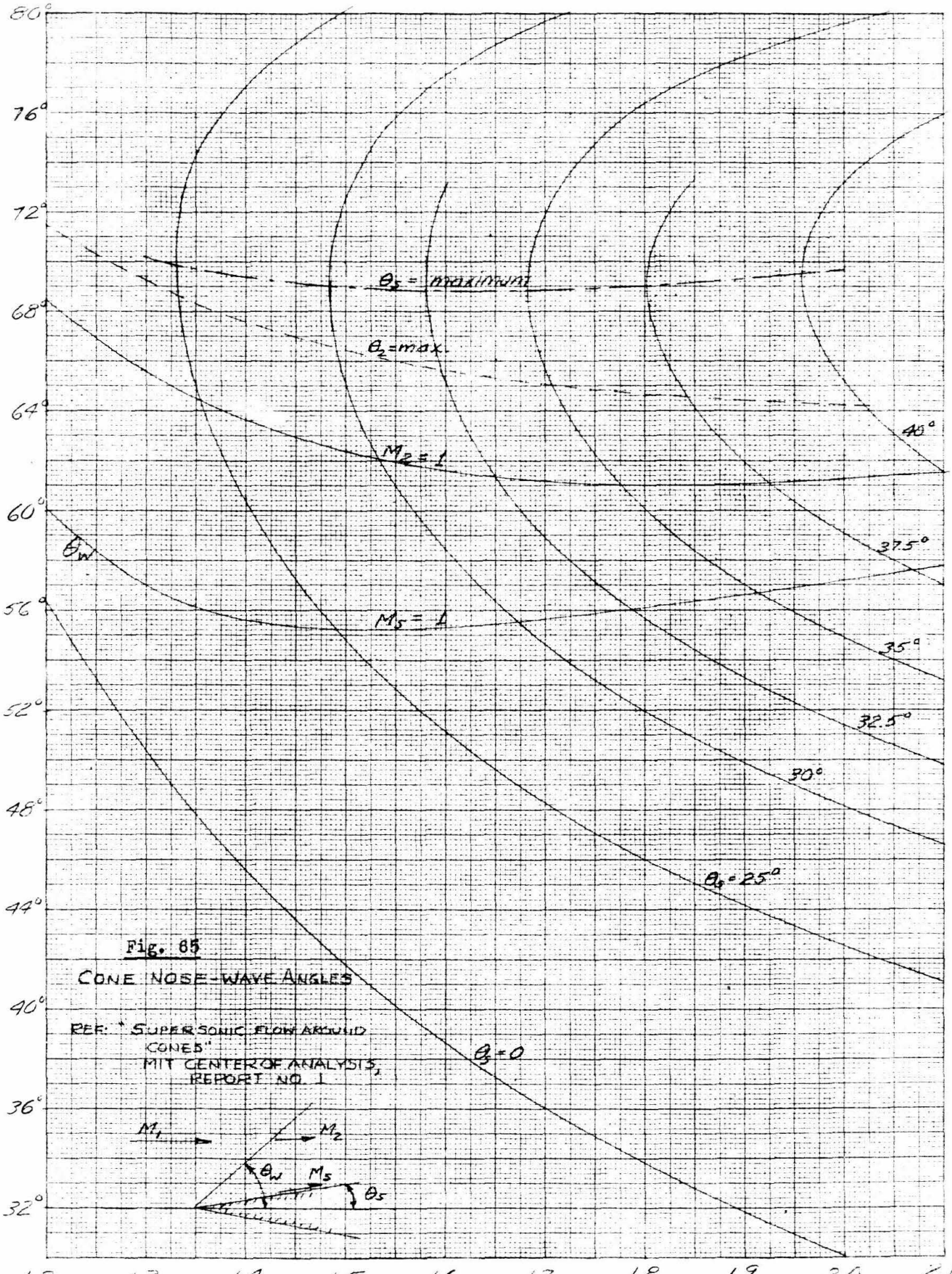

Fig. 65

CONE NOSE-WAVE ANGLES

REF: "SUPERSONIC FLOW AROUND CONES" MIT CENTER OF ANALYSIS, REPORT NO. 1